Technische Universiteit
Eindhoven
University of Technology

Electromechanics & Power Electronics
Department of Electrical Engineering
Den Dolech 2, 5612 AZ Eindhoven
P.O. Box 513, 5600 MB Eindhoven
The Netherlands
w3.ele.tue.nl/epe/

Concept study of 20 MW high-speed permanent magnet synchronous motor for marine propulsion

Author:
Dipl. Eng. M.D. Bogomolov

TU/e supervisors:
Dr. J.J.H. Paulides
Dr. A. Borisavljevic
Prof. dr. E.A. Lomonova

Date
22.01.2013

A catalogue record is available from the Eindhoven University of Technology Library

ISBN: 978-90-444-1191-1
(Eindverslagen Stan Ackermans Instituut ; 2013/009)

Abstract

High-speed permanent magnet synchronous machines are of great interest in the applications where high utilization factor and efficiency are required. Depending on application, power requirements change from kilowatts to megawatts. To investigate power limits of high-speed machines, the present feasibility study focuses on a 20 megawatt (MW) electric drive for marine propulsion. However, in addition alternative propulsion systems, ranging 100 kW to 20 MW, have been considered in an attempt to highlight some of the scaling rules that are apparent to high-speed machine considering their specific power level.

In marine propulsion, the electric drive has to provide high torque at low speed to the propeller, however at different levels due to pole towing or open water operation. For electric drives, this tends to require high frequencies (large number of poles) as well as high currents. In general, ocean-going ships exist to provide affordable transport for cargo or passengers. In this respect, there exists a range of speeds within which virtually all ocean-going ships have operated and still operate. Within this range of speeds, roughly 10-30 knots, ship propulsion speed, in revolutions-per-minute (rpm), lie within a certain range, up to a couple of hundred rpm. The horsepower range coupled with propulsion rpm makes ship propulsion motor applications a high-torque, slow-speed electric drive. To deliver 20 MW propulsion power at a rotational speed of 150 rpm requires almost 1,300,000 newton meter (Nm) of torque. Emerging ship designs that employ different propulsion, e.g. water jets, may change this. However, in the following decades, ship propulsion motors will remain to be dominated by high torque, slow-speed motors, which are likely to remain for quite some time yet. In this respect, state-of-the-art ship propulsion motors are almost entirely alternating current (AC) synchronous wound field water cooled motors, or AC asynchronous induction motors.

This report aims to give a general introduction to the concept of electrically-propelled vessels and presents specifically a feasibility study to a 20 MW high-speed permanent magnet synchronous motor (PMSM) to be used for ship propulsion. Although that also an initial attempt is documented to provide scaling laws for high-speed PM motor ranging from 100 kW to 20 MW. The purpose of this report constitutes a concept study and not an in-depth system analysis that would be required when implementing this technology for an electrical drive in future propulsion systems, such as ships or large vehicles. However, special attention is given to the apparent design challenges for these large high speed electric drives and their possible solutions.

Acknowledgments

My first words of thanks I would like to address to the Chair of Electromechanics and Power Electronics Group at TU/e, prof. Dr. Elena Lomonova, for her guidance, constant support and encouragement during my PDEng training. I am also deeply grateful to her for the opportunity to work on this project.

I would like to thank the Director of Postmaster Designer Program SAI-ICT, prof. Dr.-Ing. Leon Kaufmann for the possibility to perform my two year PDEng training.

I want to express my gratitude to my supervisors, Dr. Johan Paulides and Dr. Alexandar Borisavljevic for their thoughtful guidance and valuable advices during the course of research. I would also like to acknowledge Dr. Frans Thoolen from CCM B.V.[1] and prof. Dr. ir. Tom van Terwisga from MARIN[2] for sharing their knowledge and experience in the fields of mechanical and marine engineering.

I am indebted to my beloved family and, especially, to my dear Sasha for their support, understanding and believe in me.

[1] CCM, which stands for Centre for Concepts in Mechatronics, is a company located in Nuenen, the Netherlands.

[2] MARIN stands for Maritime Research Institute Netherlands. Location of MARIN is Wageningen, the Netherlands.

Contents

List of Symbols

Symbol	Unit	Description
$\hat{A}$	[A/m]	Peak value of the fundamental wave of electric loading
A_d	[m^2]	Heat dissipation area
$\hat{B}$	[T]	Peak value of the fundamental wave of magnetic flux density
D	[m]	Pitch circle diameter
D_r	[m]	Rotor diameter
D_1	[m]	Diameter of the driving gear
D_2	[m]	Diameter of the driven gear
δ_{eff}	[m]	Effective air gap length
DP	[m]	Gear diametrical pitch
E	-	Young's modulus
F	[m]	Gear facewidth
g	[m]	Air gap length
I	[A]	Current
I	[m^2]	Second moment of inertia
k	-	Safety factor
k_w	-	Winding factor
L	[H]	Phase self-inductance

l	[m]	Length of the bar
l_{max}	[m]	Maximal rotor length
L	[H]	Synchronous inductance
l_s	[m]	Rotor length
λ	[W/(m·K)]	Thermal conductivity
μ_0	[Wb/(A·m)]	Permability of vacuum
M	[H]	Mutual inductance
m	-	Coeffecient defining heat dissipation area
n	[Hz]	Rotational speed
n_{max}	[Hz]	Maximum rated speed
N_a	-	Number of teeth on a ring gear
n_l	[Hz]	Rotational speed of a carrier
N_p	-	Number of teeth on a planet gear
n_p	[Hz]	Gear rotational speed
N_s	-	Number of teeth on a sun gear
n_s	[Hz]	Rotational speed of a sun gear
P	[W]	Power
P	[N/m^2]	Pressure
p	-	Number of pole pairs
P_{cu}	[W]	Copper losses
P_{max}	[W]	Maximum rated power
P_m	[W]	Cylinder internal pressure
Q_s	-	Number of slots

ρ	[kg/m^3]	Material density
R_i	[m]	Inner radius
R_{th}	[(m^2·K)/W]	Thermal resistance
S	[m^2]	Area of the cylinder cross-section
σ	[N/m^2]	Shear stress
σ_h	[N/m^2]	Hoop stress
σ_{max}	[N/m^2]	Maximal stress
σ_m	[N/m^2]	Stress caused by magnet pressure
σ_s	[N/m^2]	Stress caused by rotation
σ_{tot}	[N/m^2]	Total stress
σ_T	[N/m^2]	Stress caused by thermal expansion
T	[N·m]	Electromagnetic torque
t	[m]	Thickness of the cylinder
τ_p	[m]	Pole pitch
Θ	[K]	Average temperature change
V_r	[m^3]	Rotor volume
w	[rad/s]	Angular speed
w	[m]	Width of the bar
w_m	[rad/s]	Machine mechanical angular speed
w_1	[rad/s]	Angular speed of the driving gear
w_2	[rad/s]	Angular speed of the driven gear
X_d	[Ohm]	d-axis reactance
X_q	[Ohm]	q-axis reactance

Acronyms

Acronym	Description
AC	Alternative current
AIM	Advanced induction motor
CAD	Computer-aided design
CPP	Controllable pitch propellers
DC	Direct current
EMF	Electromotive force
EPS	Electric propulsion system
FEM	Finite-element method
FPP	Fixed pitch propellers
HTSC	High temperature superconducting
ICE	Internal combustion engine
IGBT	Insulated-gate bipolar transistor
IM	Induction motor
IMO	International marine organization
IPS	Integrated power system
LNG	Liquified natural gas
MCR	Maximal continuous rate

POD	Propulsion with outboard drives
PM	Permanent magnet
PMS	Power management system
PMSM	Permanent magnet synchronous motor
PWM-VSI	Pulse-width modulation voltage source inverter
rpm	Rotations per minute
SC	Supercavitating
SFOC	Specified fuel oil consumption
WFSM	Wound field synchronous motor

List of Figures

List of Tables

Chapter 1

Introduction

The main driving factors for electrical marine propulsion units are low mass and volume, low noise and vibration, and reliability. Numerous research studies have been conducted on various electrical motors for marine propulsion, mainly AC synchronous (wound field), AC induction motors, superconducting motors, radial and axial permanent magnet motors, and some on transverse flux permanent magnet motors. All these advanced motor technologies, to be widely applied to oceangoing ships, must, though, become cost competitive and reliable with the presently extremely reliable and durable propulsion technologies. On strictly a motor-to-motor or motor-to-ICE (Internal Combustion Engine) comparison, the advanced motor technologies should be 50-75% less massive and occupy 20-70% less volume than the state-of-the-art motors. This would provide worthwhile improvements at the ship's power system level.

1.1 Motivations and objectives

Electrical propulsion (EP) in marine sector is a technology that has been under development for decades. However, only recently it was proven by empirical data, based on shipowner's experience, that exisitng on- and outboard electrical drives can bring significant benefits, particulary in the terms of fuel savings. The advantages of electrical propulsion systems have encouraged electrical machine manufacturers to draw a considerable attention to the marine industry. A brief market research gives a clear insight into the intensity of the EP implementation. For the last decade a great number of the multimillion contracts have been signed between shipbuilders and electrical power systems producers. The world largest motor producers, such as ABB, Converteam, GE, Siemens, etc. have divisions providing solutions specifically for the marine applications. Since 2008 Daewoo Shipbuilding and Marine Engineering (DSME) and Samsung Heavy Industries have been delivering liquified natural gas (LNG) tankers with installed EP systems [1]. DSME is currently constructing two pipeline installation vessels equipped with diesel-electric drive for Petrobras [2], while Samsung has recently ordered a STADT AS electrical propulsion system [3].

Mentioned above shows huge prospects of marine electrical propulsion market. Development and patenting of new disruptive solutions in this field can bring tremendous

benefits to the patent holder in the future. This was a main motivation for a customer to carry out research in the field of electrical marine propulsion and cooperate with Eindhoven University of Technology in the framework of author's PDEng final project.

Most of the electrical drives, which are presently produced for the marine industry, employ low-speed synchronous or induction motors. Although high-speed high-power permanent magnet motors recently appeared on market [4] and showed a huge potential for the megawatt applications, there was a little research carried out in the field of application of high-speed permanent magnet machines for ship electrical propulsion. Considering that such solution can bring significant advantages over the existing ones and might be patented, a nine months research was carried out by the author in cooperation with customer. This report describes the performed work.

The main goal of this report is to provide a design of a 20 MW high-speed permanent magnet electrical motor, which can be used for ship propulsion. The proposed motor should have advantages over existing ones in the terms of size and mass. Considering that state-of-art motors of the same power have mass of some 100 tonnes, the estimated mass of the designed motor should be not higher than 40 tonnes. It should have maximal possible rotational speed, which can be reached by this class of machines. The design should include geometrical as well as operational characteristics of the motor. Description of the design challenges, trade-offs and possible solutions should be also included in the report. Additionally, it should be shown how down scaling of the motor rated power affects the design trade-offs. The second goal of this report is to explore possibilities for patents in the field of application of high-speed electrical motors for ship propulsion. This assumes development and assessment of different drivetrain configurations that employ high-speed permanent magnet machines, and calculation of gearbox (mechanical or magnetic) that is required to match a motor speed to the propeller speed. It should be analyzed and explained why it is assumed that proposed drivetrain configurations have advantages over existing ones in terms of compactness or efficiency. However, in-depth analysis of the propulsor hydrodynamics should not performed. Only the first-order estimation of the hydrodynamic losses (if such are present), experienced by the proposed drivetrain configuration, is sufficient.

1.2 Contribution to the company and society

The main value that is added by this report to the company is that it presents innovative solutions in a such conservative sector as a marine industry. It shows the prospects and possible road-map of marine propulsion development, and also presents a look of electrical engineer to the area that is mostly dominated by mechanical experts. Only having knowledge about recent developments in the electrical machine design, it is possible to propose new ideas for the marine electrical propulsion, as it was done in this report. The obtained solutions are highly evaluated by the companies so as they might bring solid advantages in the race for the new technologies and new market opportunities.

1.3 Strategy

Fig.1.1 illustrates project strategy. As an introduction to the topic, a general research on marine propulsion was carried out. Different types of ship electrical propulsion were reviewed, and a brief description of electrical motors used for ship propulsion was given.

In order to provide a design of a high-speed megawatt electrical motor, design challenges were firstly reviewed and assessed. The possible trade-offs were presented and possible solutions were analyzed. To establish initial requirements and check design boundary conditions, empirical data from electrical motor manufacturers was used. In a first order approximation it was assumed that the maximal rated speed of 20 MW motor is 10,000 rpm. Based on the empirical data, obtained form experts in mechanical engineering, maximal thickness of a magnet enclosure was chosen as 3 cm. Once the initial parameters had been defined, an algorithm, implemented in Matlab, was used to calculate the geometrical and operational characteristics of the motor. For electrical machine modeling, results of the author's conference publications were used [5, 6]. The electromagnetic optimization of the motor was done in the iterative way: after the motor was calculated, initial parameters were adjusted and the design were recalculated for a several times. Based on the obtained motor characteristics, a decision was made regarding further adjusting of the initial parameters. To visualize calculated motor, a 3D graphical model was built by the means of Autodesk Inventor CAD software [7].

To calculate dimensions and mass of a 20 MW gearbox that is used to match speed of the designed motor to the propeller speed, it was initially planned that empirical data from manufacturers would be used. However, because of lack of data on high-megawatt gearboxes, the data for wind turbine gearboxes of less power was used to solve specific gearbox design trade-offs. The 20 MW gearbox calculation was based on the empirical equations and fundamental laws of gearing. The typical propeller speed of a heavy vessel is in the range 100-160 rpm. Aiming to make a gear ratio integer, a propeller speed of 151 rpm was chosen as a target value. Thus, to couple a 10,000 rpm motor with a 151 rpm propeller, a gear ratio of 1:66 is required. It was assumed that a gearbox with a such ratio would consist of two stages. Initially a magnetic gearbox calculation was planned, however, because of lack of time and its complexity, only a first-order approximation of the magnetic gearbox mass was given. After the gearbox design was performed, it was investigated how down-scaling motor rated power affects previously introduced design challenges.

To develop possible drivetrain configurations, which employ high-speed megawatt machines, different types of propellers and water jets were investigated. To get insight on the hydrodynamic efficiency of a different types of propulsor arrangements, two meetings were organized with the experts in the marine field. The results of these meetings were used for a preliminary assessment of the efficiency of the developed drivetrain configurations. It was shown that high-speed motors can be used in combination with gearboxes on low-speed vessels and directly drive propeller on high-speed marine crafts. Three new possible drivetrain configurations for electircal marine propulsion were presented and shortly analyzed.

All the sketches without references, illustrated in this report, were drawn by the author by the means of Autodesk Inventor CAD software.

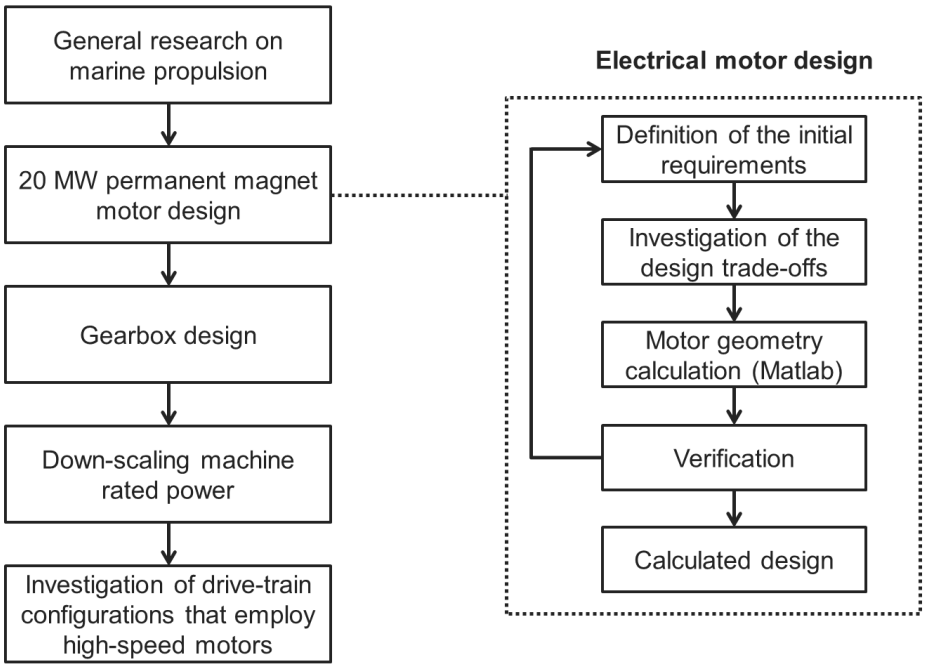

Figure 1.1: Project strategy. The right side of the figure illustrates strategy of the electrical motor design.

1.4 Report outline

The report has the structure as follows:

Chapter 2 provides a general introduction to the electrical marine propulsion. The advantages of EP systems are represented and analyzed. Different types of electrical propulsion are reviewed and the main issues of a ship power system design are represented.

Chapter 3 focuses on the description of electrical motors that are used for marine applications. The special attention is paid to the concept of high-speed megawatt motor.

Chapter 4 is dedicated to the issues of a high-speed electrical motor and a gearbox design. It introduces design challenges, trade-offs and possible solutions. In the conclusion of the chapter, the calculated design data for 20 MW 10,000 rpm motor and 20 MW gearbox is given.

Chapter 5 describes how a down scaling of machine rated power affects high-speed machine design challenges, and presents calculated design data for 100 kW 10,000 rpm motor.

Chapter 6 introduces the possible ship drivetrain configurations that employ high-speed motors.

Chapter 7 presents a general conclusion of the report and discusses the future research issues.

Appendix A contains a project baseline document.

Chapter 2

Introduction to the Electrical Marine Propulsion

To distinguish the various marine propulsion concepts, the term *electrical propulsion* will be referred to the systems that use electrical energy to transmit propulsion power from the prime mover to the propeller. The term *prime mover* is used with regard to the unit that provides power for the vessel. Correspondingly the term *mechanical propulsion* assumes that the power is transmitted to the propeller only via mechanical components. A short comparison between these propulsion concepts is given below.

2.1 Advantages of electrical propulsion

Diesel engines and gas turbines are currently the dominant propulsion systems in marine applications. However, advances in power electronics and electrical motor technology, enabled the implementation of electric propulsion on ships. EP offers the following advantages compared to the conventional mechanical systems [8, 9, 10]:

- Higher payload.
- Greater ship design flexibility.
- Higher reliability.
- Increase in fuel savings.
- Reduction of maintenance costs.
- Increase availability of auxiliary power.

Nowadays, electrical propulsion is considered a standard for cruise ships and is ever more implemented on icebreakers, service vessels (aeronautic, research, pipe-laying) and offshore drilling platforms [9, 11, 12]. Increased investment costs brought by EP are still a breaking factor for its implementation on cargo vessels, bulk carriers and chemical tankers. However, there is a significant amount of factors that stimulates the use of EP. Among them the following can be distinguished:

- Comparatively short payback time.
- Increased requirements set by International Marine Organization (IMO) to emission reduction (Fig. 2.1).ropulsion for ships
- Advances in technologies of electrical drives.
- Increased oil prices, which is generally reduced by minimizing the vessel's average speed.
- Positive feedback of owners of vessels equipped with EP.

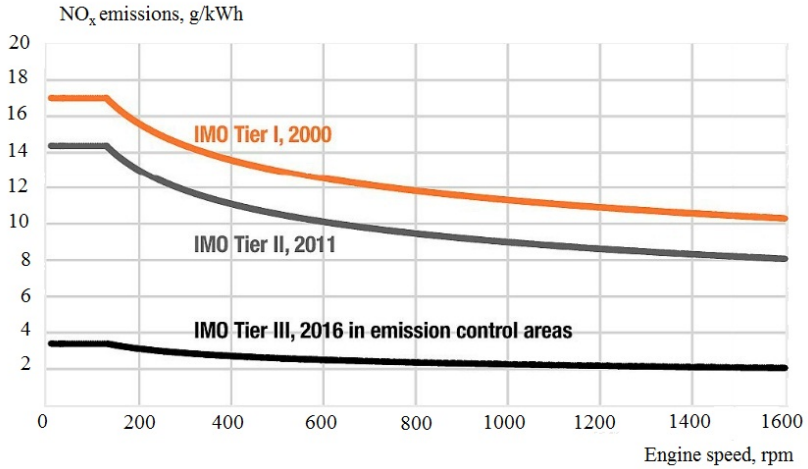

Figure 2.1: IMO exhaust emission regulations [13].

2.2 Fuel consumption and power efficiency

A direct-drive diesel driven propulsion system consists of a diesel engine, shaft and propeller. Depending on the engine speed, a reduction gear has to be employed to match the propeller speed requirements. If power burst or high level of redundancy is required, additional engines or turbines are connected to the shaft via clutches, gears with variable ratio and other auxiliary mechanical components. Compared to the direct-drive diesel driven propulsion system, EP introduces additional losses. More specifically, the EP system power flow passes through a generator, switchboard, transformer, power converter and motor (Fig. 2.2). During this conversion, about 10-12% of the energy is lost. However, physical decoupling of the propeller from the prime mover allows for a more efficient and constant speed use of the diesel engine. This gain, brought by an increased efficiency of the prime mover(s), makes the whole diesel-electric system more efficient compared to its direct-drive diesel driven counterpart.

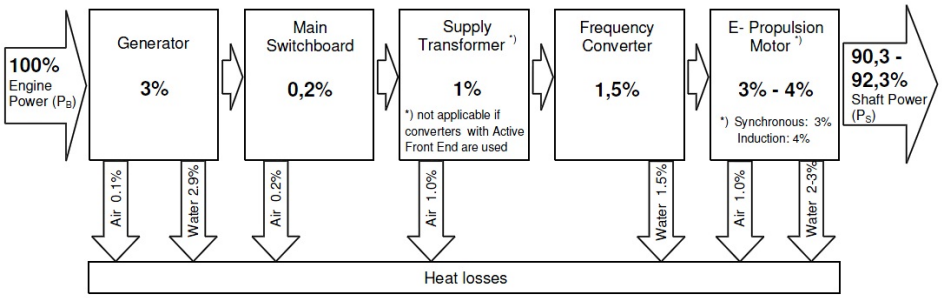

Figure 2.2: Power losses of an electrical propulsion system [8].

The hydrodynamic efficiencies of an EP and a mechanical system differ significantly. To achieve a high degree of maneuverability, improve diesel engine efficiency and optimal speed operation, controllable pitch propellers (CPP) are often used in mechanical propulsion [14]. Electrical propulsion allows for the use of variable speed fixed pitch propellers (FPP). Besides the cost difference (CPP may be up to 3-4 times more expensive compared to the FPP), at low load conditions the hydrodynamic losses brought by the CPP are estimated as 15% [15], while for the FPP the losses are almost zero. If a podded system is implemented, the propeller position is set to achieve the maximum possible hydrodynamic efficiency. This is different from the diesel propulsion, where the propeller position is defined by the mechanical restrictions brought by the position of the prime mover, which is illustrated in Fig. 2.3.

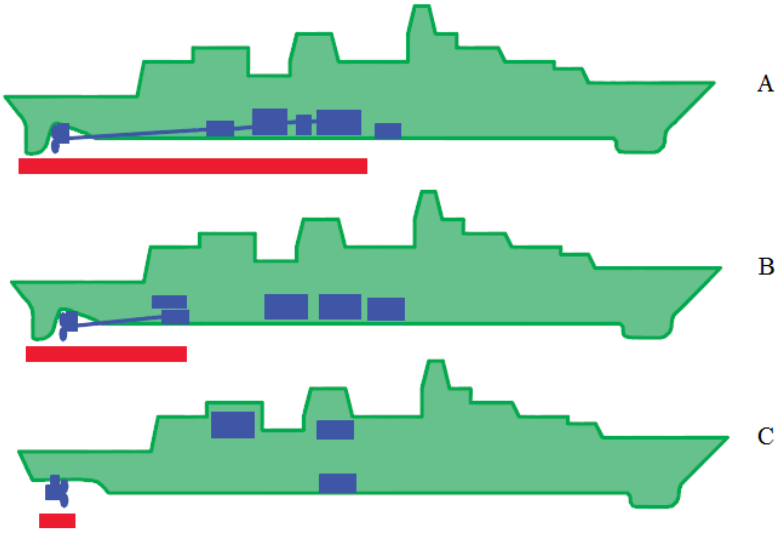

Figure 2.3: Layouts of mechanical (A), electrical (B) and electrical podded (C) propulsion systems [11]. The drivetrain components are highlighted with blue color. Red line under the ship shows the space needed for mechanical transmission. Note that in C the pulling type of propulsion is used, which significantly increases hydrodynamic efficiency.

As shown in Fig. 2.4, diesel engine operates with maximum efficiency at approximately 70% of maximal continuous rate (MCR) power mode. Different engine control strategies, as well as mechanical tuning can shift the point of the maximum efficiency.

However, Fig. 2.4 shows a common feature of diesel technology, namely that engines have maximum efficiency only in a relatively narrow range of the output power. Efficiency of electrical motors deviates much less in the range from zero to rated power. Taking into account that most of the ships spend only a small fraction of its lifetime at full power, fuel consumption of a diesel-electric set is less compared to a directly driven diesel propulsion unit. Figure 2.5a illustrates engine operational time in different mode while Fig. 2.5b shows total fuel consumption. As can be seen from both figures most of the engine service time and fuel is spent in non-optimal mode.

The main reason that does not allow directly driven diesel propulsion units to operate constantly in high-efficiency mode is the variation of the ship's power demand. The sharp profile of the propulsion load, experienced by a vessel, is typical for icebreakers, supply vessels and cruise ferries. This makes EP systems especially beneficial for this kind of ships. According to [15], for a field vessel support, the fuel savings of the diesel-electric drive are estimated as 700 tonnes per year, which is equal to $ 927,000 based on the average marine diesel price on 20th August 2012. According to [9], a navy ship, equipped with EP, can save up to 25% of fuel. As dated by different shipowners, in vessels with a diversified operational profile fuel savings up to 30-40% are achieved, [15].

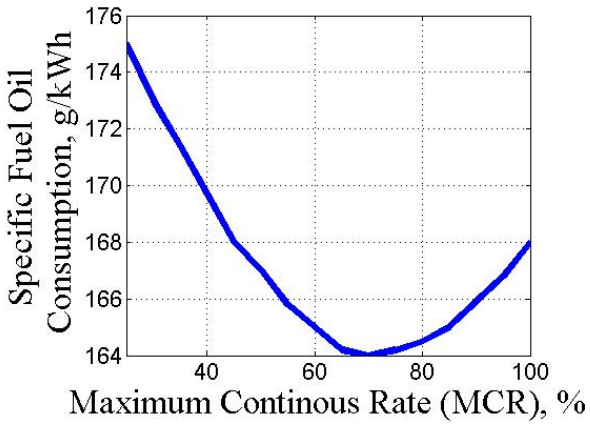

Figure 2.4: Diesel engine efficiency in the different power modes. SFOC stands for specific fuel oil consumption while MCR stands for maximum continuous rate. The data is given for the 25 MW standard engine 6S80ME-C8.2 produced by MAN [16].

2.3 Vessel payload

By eliminating the mechanical restrictions of the direct-driven diesel engines, the various components of the electrical propulsion system can be placed at locations that offer the most efficient ship packaging (Fig. 2.3). The propulsion set room configuration can be chosen accordingly to the actual volume occupied by the components; the size penalties brought by long shaft and restriction for engine placement are avoided. As an example, in EP systems the prime movers can be located higher in the ship, and thus, the ventilation ducts become shorter and occupy less space. Vibration and noise produced by electrical motors are much less compared to diesel engines. Moreover, motors do not

produce exhaust gases. Therefore, in cruise ships the cabins can be located closer to the propulsion room.

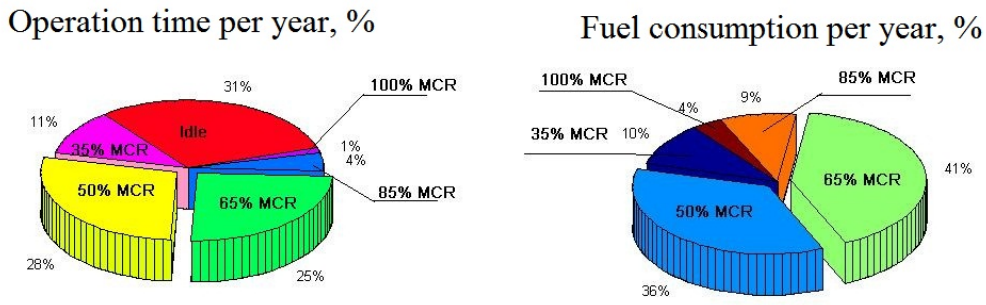

(a) (b)

Figure 2.5: Different modes of engine operation: a) Service time b) Fuel consumption. Derived from [16] for the ship equipped with 25 MW standard engine 6S80ME-C8.2 produced by MAN. MCR stands for maximum continuous rate.

In the marine industry, mainly two-stroke diesel engines are installed. The power-to-mass ratio of two-stroke diesels is much lower compared to four stroke topology, which can be used to provide mechanical power for generators in EP (Fig. 2.6a). Calculating the mass of the propulsion set, one should keep in mind that a low-speed diesel is normally equipped with a long shaft, while in EP systems a medium speed engine is coupled with generator. Thus, it would be reasonable to compare power-to-mass ratio of two drive sets: diesel engine, equipped with shaft, and a genset. Figure 2.6b shows that the power density of the genset is significantly higher compared to the engine and "long" shaft used in the directly driven diesel configuration. The reduced fuel consumption results in reduced space needed for fuel storage (for the same range). In [9] it is estimated that when electrical drives are used, 30% volume reduction is possible compared to mechanical propulsion systems.

2.4 Electrical propulsion for naval applications

According to the announced programs and official reports, U.S. Navy and Royal Navy are highly interested and actively developing the more-electric ship technology that will suit military requirements to survivability and stealth [19, 20]. Historically, electric propulsion on navy vessels has been used mainly on submarines equipped with DC motors supplied with power stored in the on-board batteries. At present, the Virginia class submarines (SSN-774) are being equipped with electric propulsion. In 2000, U.S. Navy chose EP technology for the land-attack destroyer DD-21 after tests completed on a full-scale land-based demonstration site in Philadelphia, PA. In 2004, the first Navy's hybrid warship LHD-8 was laid down. The ship uses diesel-electric and gas-electric propulsion. The other vessel projects, which have been constructed or planned

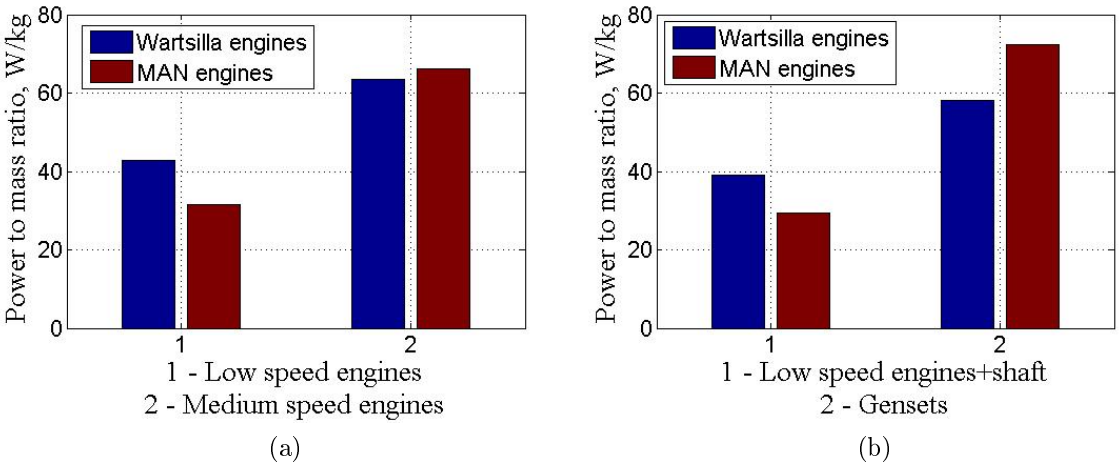

Figure 2.6: Average power to mass ratio comparison: a)Low versus medium speed diesel engines b)Low-speed diesel engines and shafts versus gensets. Derived from [17, 18].

by the Navy, include (but not restricted by) DDG 1000, T-AKE, LHD 8 and LHA 6. Currently, the concept of the electric warship is being developed for U.S. Navy with the assistance of five corporations [10]:

- Alstom, mainly working with synchronous and advanced induction motor.
- General Dynamics, focusing on PMSM.
- Newport News Shipbuilding, working on PMSM.
- American Superconductors, developing high temperature superconducting (HTSC) motor.
- General Atomics, focusing on homo-polar HTSC motor.

In 2007, Royal Navy launched "Daring", the first of Type 45 Class destroyers equipped with full-electric propulsion system. The British Ministry of Defense is currently funding the development of its own integrated power system (IPS) program. France, Germany and Italy are primarily focused on the development of electric propulsion systems for its submarines (nuclear and non-nuclear powered). The advantages brought by the EP systems for navy applications are as follows:

- Survivability.
- Flexibility of the propulsion control.
- Opportunity to optimize power system design for a given military mission.
- Increased stealth capabilities of vessels.

2.5 Electrical propulsion architecture

With the appearance of electrical drives being implemented for propulsion, the ship primary movers remain diesel engines, gas and steam turbines. However, the crucial difference between electrical and mechanical propulsion is that EP allows to redistribute power flow produced by the prime movers and to transmit it at high efficiency. This eliminates the need for long shafts and complex mechanical transmission. As such, damaged shaft will most probably stop the vessel while damaged cables from the generator to the motors could be replaced by redundant ones at reasonable costs.

An overwhelming majority of vessels require on-board electrical systems for covering service needs. In segregated power systems, propulsion power and ship service power are provided by separate prime movers. With electrical propulsion, an integrated power system can be implemented. In IPS systems, propulsion and auxiliary power are provided by the same prime movers. In past, the propulsion and electrical system of the cruise ship would require a few large diesels to rotate the propeller, and a few of medium size to supply electrical hotel load. IPS allows reducing the amount of prime movers, which increases its utilization ratio and powering density. Moreover, the total number of engine running hours and maintenance costs are greatly reduced. Besides, IPS improves controlability and reliability of the ship power system.

The concept, which is being actively developed nowadays, is an all-electrical ship. Beyond the advantages offered by IPS, in an all-electrical ship, the hydraulic and compressed air systems used for various kinds of loads are replaced with electrical drives. Moreover, if the developed concept will be standardized, the same common components could be placed on various vessels, which is clearly beneficial for the vessel design and development processes.

Similar to a land-based grid, a marine electric installation includes units that generate, convert, distribute and consume electrical power. In addition, strict requirements on safety and redundancy, over-current protection, voltage control and power management, increase the complexity of the design of electrically propelled ships.

A typical ship's power system architecture with electrical propulsion is illustrated in Fig. 2.7. However, one should keep in mind that the presented architecture is open for modifications in the accordance to the specific vessel electrical propulsion requirements.

2.6 Ship power system design

Diesel-electric plant sizing consists of several stages, which are shortly described in this section. Besides the content, the given workflow provides a clear insight into the scope of works and illustrates future research in addition to this concept study.

2.6.1 Vessel power-speed relationship

At the initial stage, the propulsion and propeller types are defined according to the vessel types and sizes [14]. Ship total towing resistance, equal to the sum of frictional,

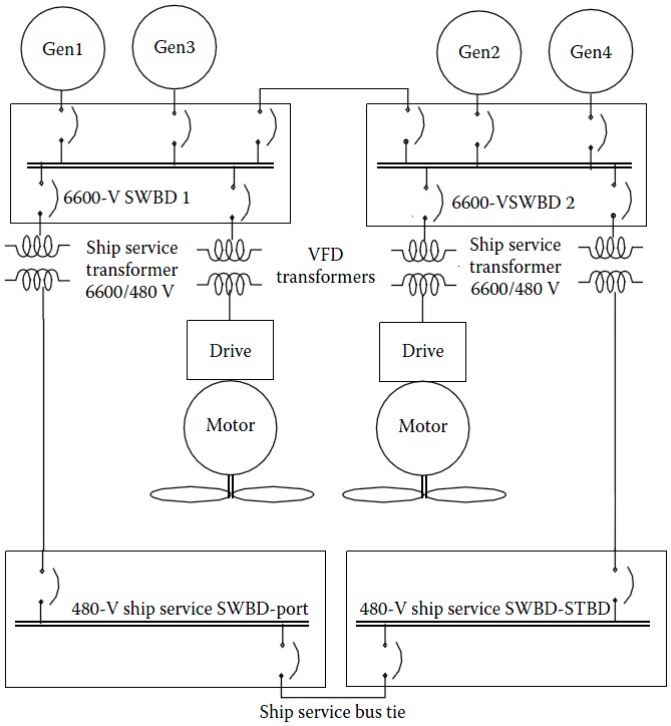

Figure 2.7: Typical ship power system architecture [9].

residual and air components, defines power, which should be provided by propeller to move ship with the required average and peak speed. As shown in Fig. 2.8, power required by the propeller is proportional to the speed cube at low speeds and to the fourth of the power at high speeds. Ship's maximum achievable speed, limited by so-called "wave wall" effect, is determined by a number of design parameters, such as hull shape and hydrodynamics. After the "wave wall", further increase in ship's power ability does not increase speed. Therefore, to move at 50% of maximal speed only 12.5% of the rated power is required. As shown, diesel engines are highly inefficient at low speed. As a result, if one aims to operate diesels in a high-efficient mode, the fuel consumption will increase greatly with only small speed gain.

Propeller design is a complicated multi-parametric task. In large ships, 4, 5 or 6 blades propellers are used. Propeller and engine load diagrams are used in a standard approach for power calculations. Numerous considerations, e.g. heavy weather conditions, require to adjusting engine power margins to cope with all possible worst-case scenarios.

2.6.2 Auxiliary electrical load

The electrical load of a ship depends on the operation mode: at sea, maneuvering, at port, etc. In modern cruise vessels, with a propulsion power of 40 MW, the hotel load can be up to 40%. For offshore construction vessels, the consumer load can be up to 25% of the total power [8]. After these preliminary electrical loads are calculated, prime movers can be sized.

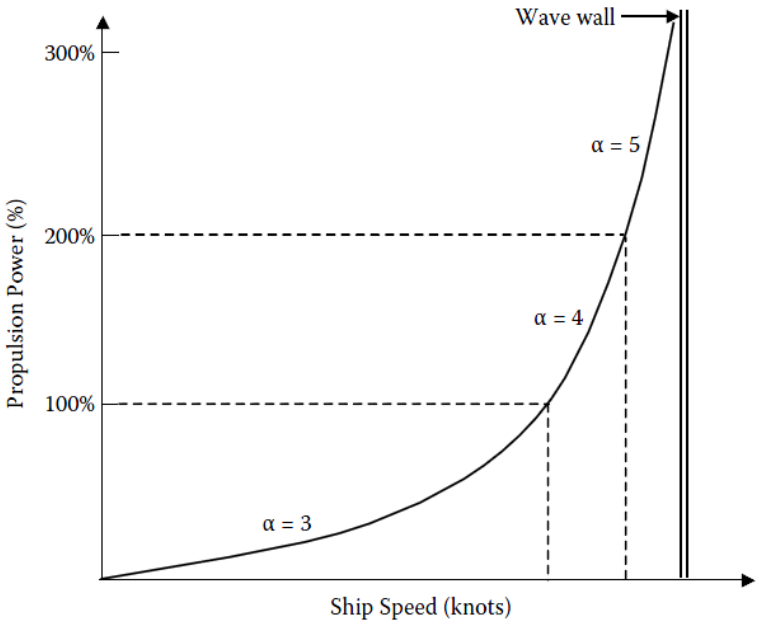

Figure 2.8: General dependence between ship speed and propulsion power [9].

2.6.3 Prime movers and generator set

As mentioned, medium to high-speed diesel engines (mostly) and gas turbines (less) are used as prime movers on most of the vessels. Diesel-electric drives are a mature technology and conventionally designed with respect to gensets and ship operational profile. Typical large power diesel-electric drives, e.g. produced by Wartsilla and MAN, have a speed of rotation of 500-1,000 rpm and generate voltage up to 15 kV [17, 18]. The generator design follows the following requirements: voltage level, availability of reactive power and total harmonic distortion.

2.6.4 Ship power distribution

The redundancy and safety requirements determine switchboard, on-board grid voltage and frequency. The over-current protection regulation forces designers to use higher voltage levels. To increase grid fault tolerance, the switchboard is divided into 2, 3 or 4 sections. If a high voltage electrical system is installed on a ship, special attention should be paid to the selection of circuit breakers to avoid sparks and arcs. To provide the required safety, the protection scheme of the ship electrical system has to be developed. Correct setting and control of the protecting devices is essential to provide a first defense against under- and over voltage, current and frequency, earth fault, thermal overload, and other fault conditions. In order to provide required isolation of different parts of the electrical power system, transformers are placed in accordance with the on-board grid topology.

2.6.5 Variable speed drives and motors

At present, about 85% of the on-board drives are used for the auxiliary systems - cranes, pumps, fans, etc. Megawatt rated motor requires powerful converters able to maintain high voltage levels and preferably high-frequency switching. To eliminate noise and vibration caused by converter harmonics, a large LC filter before the motor is required on most of ships. Due to advances in IGBT technology, PWM-VSI drives become suitable for 20 MW machines. PWM drives are advantageous due to their high power density and efficiency. Cycloconverters and load commutated inverters are widely used in large cruise ships. Compared to other type of converters, cycloconverters have the fewest number of components. Cycloconverters are used for applications where high torque is needed, e.g. icebreakers and dynamic positioning ships. Due to their large size, cycloconverters are not suitable for small ships. Moreover, cycloconverters offer a limited output frequency range and suffer from their low power factor. The selection of the suitable converter type depends on ship requirements, electrical motor type and output power/torque.

2.6.6 Power and propulsion management system

Modern power systems are highly integrated with control networks and power management systems (PMS). These are used to monitor and coordinate power generation, load and distribution. The design challenge is the selection of information management systems and user-interface, selection of centralized or distributed system level controllers, development of the philosophy and PMS configuration.

2.7 Types of electrical propulsion

Mechanical components of diesel-electric propulsion topology include shaft, propeller and rudder. A rudder is used to move the ship in transverse directions and if additional maneuverability is required, a bow thruster is installed. To avoid rudders, increase drive compactness and improve maneuverability, azimuth thrusters are sometimes installed (Fig. 2.9a). With azimuth thruster propulsion configuration, the motor is located inside the hull, and propulsion power is transmitted to the propeller via shafts and gearboxes. Depending on the motor location (horizontal or vertical) a Z- or L-type gear transmission are used. Azimuth thrusters are able to rotate through up to 360 in azimuthal direction.

The first electrically podded system (POD - Propulsion with Outboard Drives), named Azipod was introduced by ABB in 1990. Pod is a thruster unit with encapsulated electrical motor, which directly drives the propeller (Fig. 2.9b). Compared to azimuth thrusters, pod avoids the use of a complex transmission without compromising the ability to rotate 360 degrees around its vertical axis. Complete podded propulsion systems can be delivered and fitted in days, thus avoiding the lengthy installation of a conventional propulsion system. The hydrodynamic efficiency is greatly improved especially in pulling type pods due to optimal and uniform wake field. Overall efficiency

of pods is claimed to be up to 15%. An improvement of conventional pod is contra-rotating propulsion system, which increases efficiency of pod up to 20% [12].

Wound-synchronous and induction motors are mostly used in pods. To date, the largest installed pod has an output power of 25 MW [21]. The important observation is that for warships, for better survivability, smaller pods are preferable, while the power provided by the propulsion system should remain. Therefore, for such applications more power-dense motors are needed, which justifies the selection of permanent magnet synchronous motors (PMSM).

(a) (b)

Figure 2.9: Examples of marine propulsion units: a) L-type azimuth thruster [22] b) Pod equipped with electrical motor [23].

Chapter 3

Electrical Motors used for Marine Propulsion

3.1 Propulsion electrical drive configuration

In many applications, the demand for compact and efficient electrical drive systems has created an opportunity for high-speed machine use. In these applications, permanent magnet (PM) machines are recognized as a favorite, due to their high power density, relatively simple construction and high efficiency. Several extremely high-speed PM machines have been reported, both on the market and in academia, with speeds up to 1,000,000 rpm. However, for ship propulsion this has not been thoroughly researched yet due to the necessity of gearing both the speed and the torque. For example, in industry machinery operates at greatly different speeds. A large cement mill or steel converter runs at fractions of a revolution per minute, while centrifugal compressors operate at 5,000 to 20,000 rpm. In between these extremes, the large majority of machines are running at 10 to 1,000 rpm. The absorbed powers vary as widely, from fractions of a kilowatt to many megawatts for ship propulsion. In this respect, gearboxes are used to match the operating speed of the prime mover to the requirements of the propeller. As such, they will be used as speed increasing or decreasing drives. Conventional gearboxes come in all sizes and ratios, transmitting a few watts in power tools to 50 or 60 MW in ship propulsion and gas turbine driven generators.

The combination of high-speed motors and gearing is well known for power tools. These drives, up to some kilowatts power at 20 to 30,000 rpm, do not pose problems for either gearing or bearings, and are well established technology. The advent of cost-effective frequency converters has allowed the speed range of larger induction motors of 100 to 1,000 kW to be increased to 4,000-6,000 rpm. The prospect of a permanent magnet motor of 20 MW operating at higher speed offers the possibility of low mass, very compact geared or direct-drive, which have been used at these higher speeds for decades, i.e. in combination with both steam and gas turbines.

3.2 High-speed electrical machines

The boost in speeds of PM machines is linked with overcoming or avoiding a number of machine limitations. Various physical parameters (stress, temperature, resonant frequencies) can limit the speed of an electrical machine. Aside from speed, these variables are also affected by power, size and machine electrical and magnetic loading. The tangential speed at the outer rotor radius is often taken as a criterion when defining high-speed because it also takes into account the size of a machine. High-speed machines are classified according to operating power and rotational speed. A numerical limit is proposed in this report that correlates the power limit with the rotational speed of an electrical machine.

3.3 Power electronics

The rapid development in marine propulsion has a significant thrust towards the use of electrical propulsion and the integration of auxiliary and propulsion power systems, where the need for very flexible, robust and compact power systems is ever increasing. This need is going to be satisfied through recent advances, verging on revolution, in power electronic device construction, and their application for power conversion and control. Further, in electrical propulsion, the power is provided by generators to the propulsion motors. Therefore, the ship constitutes an island grid, hence active power to frequency and reactive power to voltage balances have to be matched, fluctuations are also allowed other than in onshore grids, where enough control reserve has to be provided to keep the frequency and voltage nearly constant. So, system stability is a relevant concern in island installations. Modern AC to AC power conversion systems offer the advantage of compact, efficient and bi-directional power modulation for ship drives in the range of 2.6 to 4.5 MW.

The recent developments in switching device implementation have been fundamental to the developments underway in marine electrical power systems. The application of multilevel inverters has been very attractive for medium to high voltage range (2 to 13 kV) applications such as: motor drive systems, power distribution, power quality and power conditioning applications. The ability to apply these new techniques to hybrid electric drives for ships results in hardware selection that allows very low harmonic distortion of the output waveforms and consequent smooth operation over the entire speed range.

3.4 Electrical motors for marine propulsion

Generally, the selection of the motor for electrical propulsion is based on the preference of the shipbuilder, since different motor types have different advantages and disadvantages. Moreover, one can notice that different manufacturers promote their own solutions as the best suitable for marine application. Hence, the motor selection depends on the motor producer's reputation. For example, ABB has installed more than

120 pods with induction motors, while Siemens is concentrated on the high-temperature superconducting and permanent magnet synchronous motors.

The specific motor requirements to marine applications can be classified as follows:

- High reliability.
- High compactness.
- High shock-resistance.
- Low power consumption.
- Low emission.

Based on reports, industrial experience and performance characteristics of the available motors, the following types should be considered as candidates for the ship propulsion:

- Induction motors.
- Wound-field synchronous motors.
- High-temperature superconducting (HTSC) synchronous motors.
- Permanent magnet synchronous motor.

3.4.1 Induction motors

Induction motors (IM) offer robust design and comparatively low costs. It is a mature technology and most widely used in the heavy industries. IM have been used for decades in marine applications and have been installed on a large amount of vessels in different configurations. Advances in IGBT technologies have assisted in the production of efficient converters. A possibility to connect multi-phase (12 to 15) high-power machines, controlled by PWM-VSI drive, directly to the converter without transformers is a great advantage in terms of mass and cost reduction. However, even the most efficient IM installed nowadays are comparatively heavy and occupy a lot of space. For example, a 20 MW 180 rpm advanced induction motor (AIM), produced by Converteam, has a mass of some 100 tonnes [24].

3.4.2 Wound-field synchronous motors

According to [25], wound rotor synchronous AC motors are the most used structure in ship propulsion for the last decade. Wound field motors are more efficient than induction motors. However, the excitation system of the motors requires additional space. Therefore, compared to permanent magnet synchronous motors, the power density of wound rotor motors is lower. The wound-field motors are a reasonable solution for commercial vessels, however, for navy applications and pods more compact solution are preferred.

3.4.3 High-temperature superconducting motors

Since the 1970s high-temperature superconducting materials have been investigated. In this respect, high temperature refers to 30-40 K, which is much higher than 5 K - a normal temperature when superconductance is reached [26]. American Superconductor Corporation has built and tested a 36,5 MW, 120 rpm motor [10]. The mass of such a motor is some 75 tonnes. GE initiated the development of a 100 MW generator that employs an HTSC field winding. During the last decade the technology of HTSC has become commercially available, however, this technology is still under development and testing.

The key feature of the superconducting motor is the additional cryogenic equipment to cool the conductors below the temperature when the effect of superconductance takes place. The small resistance of superconductors allows the current density to be up to 100 times compared to conventional machine. Thus, potentially HTSC offers the highest power density and energy efficiency. However, one should keep in mind that the cooling equipment poses an additional technical risk and notably increase the costs of the system.

3.4.4 Permanent magnet synchronous motor

The permanent magnet synchronous motor (PMSM) offers a high power density at reasonable costs. Fig. 3.1 illustrates the efficiency of high-power induction motor compared to a PMSM. The PM motor efficiency can reach values of 98% while the efficiency of induction motors is limited to 94-96% at full load. However, at part load the PMSM motor clearly shows its advantage. PMSM are less affected by rotor current loss, less noisy and much more compact compared to IM. Although that the main disadvantages of PMSM are magnet costs, magnet sensitivity to high temperature and partial demagnetization.

To summarize, Table 3.1 shows the key features of different motor types suitable for marine propulsion.

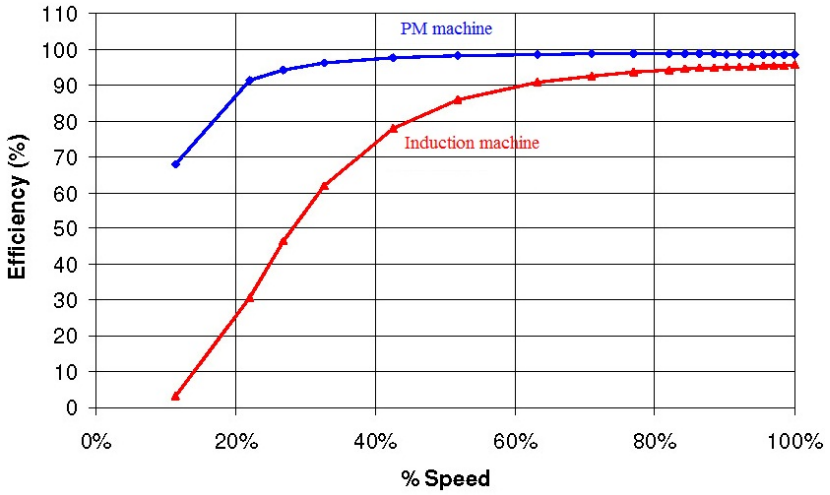

Figure 3.1: Comparison of efficiencies of PM and induction megawatt machines. One should note that the efficiency of synchronous machines is similar to the efficiency of induction machines. The figure is based on the data provided by Advanced Electromagnetics B.V. [27].

Motor type	Advantages	Disadvantages
IM	Robust, relatively cheap and simple.	Low efficiency, low power density.
Wound rotor	Compared to IM more shock resistant because of larger air gap, have higher efficiency and power factor.	Need separate winding excitation; brushes and slip rings add complexity and maintenance costs.
PMSM	High power density, low noise, maximum torque at zero speed.	Thermally sensitive, operation at high speeds needs rotor enclosure.
HTSC	Offer potentially highest power density and energy efficiency.	Need complex cryogenic equipment. Non-mature technology. At present date only a few large-power machines exist.

Table 3.1: Brief comparison of the motors to be used for ship propulsion.

3.5 Conclusion

Concept of megawatt high-speed machine

Present low-speed permanent magnet motors have reached powers of 65 MW [28]. At the same time, high-speed permanent magnet synchronous motors (PMSM) have been used in a great variety of applications and achieve speeds of up to 1,000,000 rpm [29]. Although the design of megawatt high-speed machine is still a challenge, such machines have become commercially available [4], and are currently used mainly in oil & gas and petrochemical industries.

Electrical propulsion in the marine sector is an emerging technology offering a wide area for the future research and development. Progress observed in PMSM technology coupling with long-term costs benefits gives a promising topic for research of permanent magnet motors installed in ship propulsion systems. Use of high-speed PMSM offers increased efficiency and compactness compared to most currently implemented motors. A gearbox system is a necessary component of the drivetrain when high-speed motor is employed, however the increased mechanical complexity of geared motor is justified by the potential mass reduction, which, according to the preliminary expectations, can be up to 50% greater compared to the low-speed induction motor without the gearbox. A thorough analysis will be carried out in the following sections in order to assess the feasibility and performance of the chosen concept.

Chapter 4

Preliminary Machine Sizing

Introduction

Multi-megawatt high-speed PM machines are characterized by a robust rotor construction since they are typically speed-limited by the strength of the materials chosen. This narrows the rotor topology of choice to a surface-mounted or embedded magnet construction [30, 31]. The non-magnetic sleeve, illustrated in Fig. 4.1, is used to achieve necessary mechanical retention of the surface magnets, which increases the effective length of the air gap, and, therefore, decreases flux density for a given magnet height. Embedded magnets do not need any external enclosure, however, experience higher interpole flux leakage, which also decreases maximum achievable air gap flux density. Because of the advantages related to the manufacturing process and simpler analytical description, the surface mounted magnets are selected for the current design.

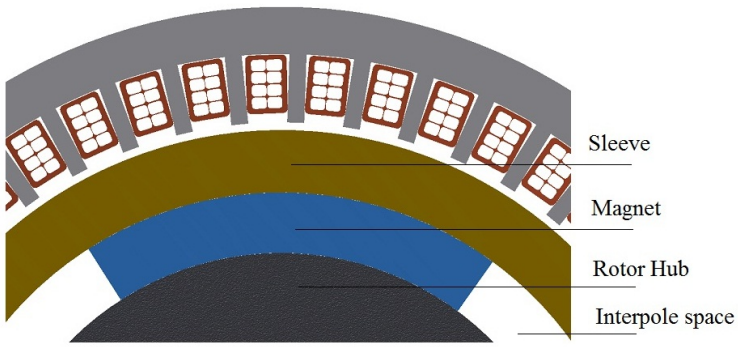

Figure 4.1: Layout of PM motor with surface-mounted magnets and carbon sleeve. The figure is a front view of a 3D model built by the means of CAD software.

The basic rotor arrangement types are the following: exterior, interior and double rotor. Exterior rotor could be more compact because of the higher radius, and, as a consequence, higher torque, compared to the interior-rotor machine of the same size. However, the exterior rotor makes cooling system more complicated. To avoid overheating, the electric loading is decreased, which diminishes the achievable shear stress. Dual

rotor machine is a novel technology, which has recently appeared on the market. Albeit dual rotor could eliminate the need for a gearbox, the machine structure becomes more complicated and less robust, which is critical for the durable operation at the high speeds for megawatt machine. Therefore, interior-rotor surface-magnet structure is selected as the most appropriate for the high-power high-speed motor.

4.1 20 MW high-speed PMSM: design challenges overview

A high speed of rotation as well as a high power rate are the reasons to pay additional attention to the following issues [4, 32]:

- Rotordynamical issues.
- Magnet enclosure design (for surface mounted magnets).
- Cooling system and motor thermal vulnerability.
- Power converter capabilities (maximum switching frequency for high voltage).
- Losses.
- Vibration assessment.
- Bearing durability.

Rotordynamical issues mainly determine the maximum dimensions of rotor. Rotational critical speeds should be considered to avoid rotor bending and excessive vibration. Surface mounted magnets do not add stiffness to the rotor, however, act as deadweights and, therefore, should be covered by an enclosure. The enclosure is usually made of non-magnetic carbon, which enlarges the effective air gap of the machine and decreases achievable air gap flux density. A high current density in the slot increases requirements to the cooling system especially when the machine surface area is comparatively low. To decrease losses occurring at high speeds, an appropriate iron type and strand configuration should be selected carefully [4]. Finally, the power converter should be able to support the necessary switching frequency at high voltage levels.

4.2 Rotor diameter, mass and rotational speed

The two basic equations linking power of the machine with its sizes are the following:

$$T = 2\sigma V_r \tag{4.1}$$

$$P = Tw \tag{4.2}$$

where T is torque, σ is shear stress, w is rotational frequency in rad/s , P is power and V_r is a rotor volume.

Coupling (4.1) and (4.2) results in the following equation:

$$P = \pi^2 D_r^2 l_s \sigma n \tag{4.3}$$

where D_r is rotor diameter, l_s is rotor length and n is rotational speed.

One should keep in mind that shear stress is dependent on the machine diameter due to the thermal restrictions. Assuming a constant number of slots and constant current density, slot current I is proportional to D_r^2. The heat generated in the slot region is dissipated through the back iron (including tooth body) and the end plates. The surface of the end plates is proportional to D_r^2, and the surface of the tooth wall is proportional to D_r. Hence, the dissipation area can be expressed as:

$$A_d \propto D_r^m \tag{4.4}$$

where $1 < m < 2$ [33].

The slot heat generation is proportional to the slot current, thus, to D_r^2. As a result of (4.4), the increase in the slot current is faster than the increase in the area of dissipation. The condition for thermal balance makes the shear stress inversely proportional to the rotor diameter:

$$\sigma = 0.5 \cdot \hat{B} \cdot \hat{A} \propto D_r^{m-1}$$

where $\hat{B}$ and $\hat{A}$ are peak values of the fundamental waves of magnetic flux density and electric loading correspondingly. According to [33] the theoretical value of m is 1.25. To illustrate the importance of the derived proportion, let us assume a machine with a rotor of 1 m in diameter and calculated shear stress of 50 kN/m^2. The machine of the same power and rotor volume with diameter of 0.5 m will have a shear stress of:

$$50000 \cdot 0.5^{0.25} \approx 42\ kN/m^2 \tag{4.5}$$

The machine output power directly depends on the rotor volume, therefore, for a first order estimation, to increase machine power one need to increase rotor volume. Apparently, the rotor volume can be increased by varying the length or diameter of the rotor. An important conclusion following from (4.5) is that for the same power increase one would need less rotor volume increase if one enlarges the rotor diameter instead of length. Hence, (4.3) might be rewritten as follows:

$$P \propto D_r^{2.25} l_s n \tag{4.6}$$

It follows from (4.3) that keeping the produced power constant, the increase in speed results in decrease of the machine volume and therefore mass. This explains why it is preferable to increase the speed of the rotation as much as possible. However, (4.3) does not show a speed limit of the machine with a given rated power. This limit is rarely

derived analytically. However, authors of [29, 34] proposed that machine maximum speed is inversely proportional to the rated power according to (4.7).

$$P_{max} \propto \frac{1}{n_{max}^3} \tag{4.7}$$

This empirical limit has been proven by GE research. Markers in Fig. 4.2 are placed according to the rated characteristics of the existing machines. Interpolating the data, one could find a line that follows the empirically established law, linking machine power and achievable speed. According to this line, it is expected that the machine of 20 MW can rotate at 10,000 rpm. Dated highest speed megawatt machine, has a power of 8 MW and rotates at 15,000 rpm.

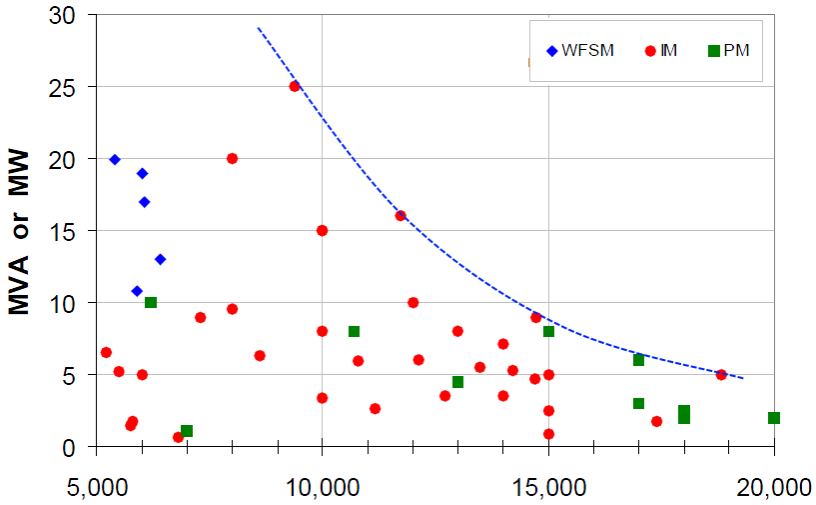

Figure 4.2: Power and speed ratings of "commercially" produced motors. Derived from [35]. The blue break line shows assumed machine power for the whole range of the illustrated speeds. WFSM stands for wound-field synchronous motor, IM for induction motor, PM for permanent magnet motor.

If to investigate only mechanical constraints of multimegawatt high-speed machines, a simple equation can be employed to estimate maximal rated power for a given speed. As it follows from [34], the maximal rotor length is calculated as follows:

$$l_{max} = \sqrt{\frac{\pi^2}{k\Omega}\sqrt{\frac{EI}{\rho S}}} \tag{4.8}$$

Where S is the area of the cylinder cross-section, E is Young's modulus, I is the second moment of inertia for a cylinder, k is , Ω is rotational frequency and ρ is material density. For a solid rotor of an electrical machine the second moment of inertia is equal to $I = \pi D_r^4/64$. The maximum rotor diameter is determined by the maximal surface speed and, therefore, l_{max} can be found. When rotor dimensions are defined, the maximal generated torque of the machine will be dependent only on the shear stress. If shear stress is taken as 50 kN/m^2, the maximum rated power of the machine is 29 MW.

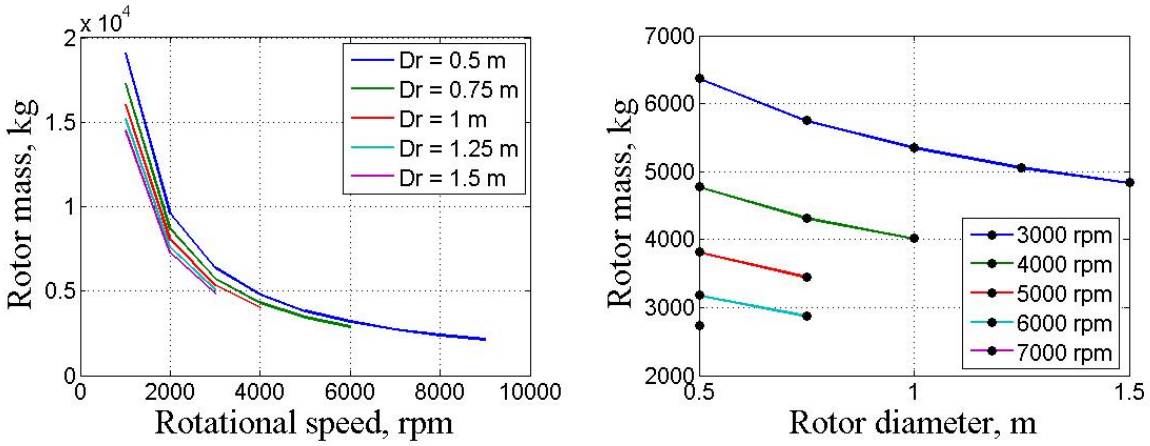

(a) (b)

Figure 4.3: Results of design calculations of 20 MW motor with 1.5 m rotor diameter and 50 kN/m^2 shear stress a) Rotor mass versus rotational speed b) Rotor mass versus rotor diameter. The maximum value of the rotor diameter for a specific speed is restricted by a maximum surface speed.

Equation (4.6) allows to estimate the potential mass reduction of a high-speed machine. Assuming that 20 MW motor with a diameter of 1.5 m has a shear stress equal to 50 kN/m^2, with increase of the rotational speed the mass of the machine will decrease as it is illustrated in Fig. 4.3a. However, Fig. 4.3a is created with the assumption that the magnetic loading is constant with speed change. In practice, because of magnet enclosure, the magnetic loading decreases. As a result, the shear stresses also decrease and, therefore, Fig. 4.3a should be treated only as an initial result. Still, it gives a clear understanding of interdependence of rotor diameter, mass and rotational speed.

4.3 Electrical machine design

Electrical machine design is a complex process that is based on the analytical assessment as well as on empirical data, finite-element modeling and experience of its designer. The iterative nature of the design calculations is stipulated by the strong interdependence of multiple design variables. Typically an existing machine is used as a template for the initial sizing. This allows designers to gradually adjust machine parameters to satisfy the posed requirements. Because of the lack of information about existing megawatt high-speed machines, there is no “template data" for the current design. As a consequence, the main motor dimensions are calculated based on well-known and proven assumptions. FEM is used to calculate strongly non-linear characteristics and verify obtained topology. The empirical data and recommendations of industrial partners play a crucial role in the assessment of the obtained results.

To clarify the design process, the following steps are distinguished:

1. The empirical data research.

2. Selection of the design variables.
3. Analysis of the constraints brought by the variables.
4. Establishment of the initial value for the parameters, based on the first three items.
5. Analytical calculation of the basic geometry and machine performance.
6. FEM results.
7. Correction of the initial values, recalculation.

An optimal design of the machine is an extremely complicated task when the number of design variables is not limited. To restrict the area of possible design solutions, a set of variables is assigned with a constant value. Such variables are defined using practical considerations, or their change does not influence the design strongly. Further, a list of "free variables" is created. The "free variables" are the variables that are independent of each other and determine the main machine dimensions and performance. Table (4.1) illustrates the design variables, its desired value and imposed constraints, which are discussed in details in the sections below.

4.4 Design variables

4.4.1 Magnetic loading

Machine dimensions. To estimate magnetic flux density, rotor dimensions should be known a priori. Fig. 4.3b shows that for a given speed the mass of the rotor is lower if the diameter is larger. At the same time, as can be seen in the Fig. 4.3b, there is a limit to the rotor enlargement for a specific speed, because of the restriction for the rotor maximum surface speed, which is taken as 250 m/s. The rotor length is calculated to avoid the first critical speed. Figure 4.4 illustrates the maximum rotor length versus diameter for various rated speeds. For a specific rated power different combinations of rotor length/diameter are possible. As a clear analytical solution for the optimum machine length/diameter ratio is hard to derive, empirical data may be referred to.

The empirical data is contradictory. According to [36], the cost of the machine is proportionally dependent on the rotor diameter. Also the end-winding to the machine length relation is lower when the rotor length is higher. However, a short rotor is beneficial from the point of view of bearing durability. Moreover, as was mentioned, slot heat dissipation is proportional to the end-winding surface. Therefore, the largest possible rotor diameter will be chosen for the design as presented in this report.

The number of poles is mainly restricted by the maximum supported frequency of the converter. Assuming that the commercially available converter "Perfect Harmony", manufactured by Siemens [37], can be used for the machine drive, the number of poles should be either 2 or 4. At the same time, the increase in the number of poles leads to a decreasing flux per pole. If the flux per pole decreases, the stator teeth can be thinner.

Design variable	Preferable choice	Issues that should be taken into account or imposed constraint
Rotor type	Surface-mounted magnets	Surface speed $<$ 250 m/s.
Rotor arrangement	Free for choice	Gearbox should be used.
Rotor diameter	High	Current loading is limited by the cooling capabilities of the machine.
Rotor length	Low	Rotor enlargement will lead to the exceeding critical speeds.
Speed	High	D_r<0.5 m
Electric loading	High	Increased requirements to the cooling system.
Magnetic loading	High	Magnet thickness, air gap and slot dimensions should be chosen correspondingly.
Number of slots	High	Given with current density and slot dimensions, defines the minimum tooth tip radius.
Slots shape	Rectangular	Winding encapsulation technology constraints.
Number of poles	Low	Constraints on magnetic design.
Air gap length	Low	Assembly mechanical constraints.
Insulation	Class F	Maximum winding temperature is 130 °C.
Sleeve thickness	Low	$<$ 3 cm

Table 4.1: Main electrical machine design variables.

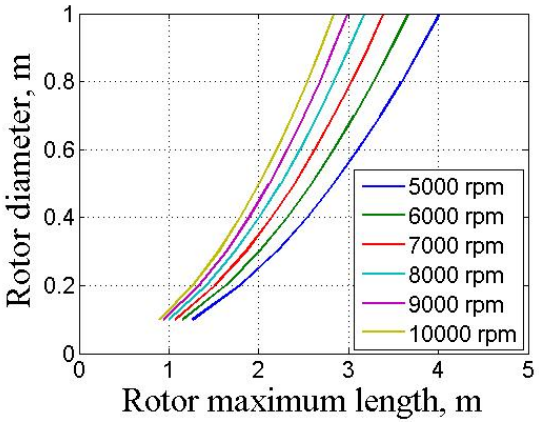

Figure 4.4: Rotor maximum length versus diameter given for the different speeds. Calculated for 20 MW machine with 80 kN/m^2 shear stress design.

As an example, doubling the number of poles decreases the yoke length by half. A small number of poles leads to a large end-winding, which is undesirable, because it results in flux penetrating the shaft.

Besides protective sleeve, magnetic flux generated by magnets passes the air gap which has a high reluctance. Although the air gap is of great significance for machine design, usually empirical equations are used to define its length. Typically, air gap length does not vary tremendously for a machine of different power. According to [38], air gap length, expressed in meters, can be defined as:

$$g = 0.0002 + 0.003\sqrt{\frac{D_r l_s}{2}} \tag{4.9}$$

However, in practice the limit for the minimal air gap length is defined by the mechanical restrictions and therefore is selected to be 4 to 5 mm. The considerations referred to the demagnetization resistance can be neglected because of comparatively thick magnet enclosure for the surface mounted permanent magnet rotor.

Sleeve calculation. To estimate the mechanical forces experienced by the rotor enclosure, well-established analytical expressions can be used. If the thickness of a rotating cylinder is approximately 5 to 10 lower than its internal radius, the hoop stress can be calculated as long as the uniform radial pressure P, occurring at its bore, is known:

$$\sigma_h = \frac{PR_i}{t} \tag{4.10}$$

where t is the thickness of the cylinder, R_i is the inner radius and σ_h is the hoop stress. Basically, (4.10) reflects the fact that for a given pressure, the cylinder should be thick enough to not exceed the maximum ultimate tensile strength of the material.

The cylinder internal pressure P_m can be calculated from the centrifugal force, produced by magnets, which act as a dead-weight. However, the inertial mass of the rotating

sleeve should be also taken into account. The maximum hoop stress occurs on the sleeve internal surface. Assuming that radial stress is zero and sleeve material is orthotropic and homogenous, the total stress occurring on the inner surface of the sleeve is:

$$\sigma_{tot} = \sigma_s + \sigma_m \tag{4.11}$$

where σ_s is the stress caused by the rotation and σ_m is the stress caused by magnet pressure.

For safety reasons, the maximum allowable stress σ_{tot} could be taken equal to 70% of the ultimate tension strength of the material. The highest hoop stress experienced by the sleeve occurs when the rotor is cold and rotational speed approaches lift-off speed. To avoid magnet detachment under these conditions, sleeve pretension is used. Considering the latter and the sleeve thermal extension, (4.11) should be modified to:

$$\sigma_{max} = \sigma_T + 2\sigma_{tot} \tag{4.12}$$

Equation (4.12) links two variables, namely sleeve thickness and magnet height. An increase in magnet height requires enlargement of sleeve thickness and, therefore, there is an optimal relation between sleeve thickness and magnet sizes in terms of maximum flux density per magnet volume and maximum achievable flux density.

Optimal magnet thickness. Magnets should have sufficient volume to keep the flux density in the air gap at the desired value. Normally, the thickness of the magnet is 5 to 10 times greater than the length of the gap [30]. Very thick magnets ($>$ 20 mm) are complex to manufacture. If the magnet width is lower than the pole pitch, the interpole space should be filled with material of a similar mass density as the magnets. The material should be non-magnetic to avoid flux leakage and non-conductive to avoid eddy currents. In large machines magnets are segmented in transverse and longitudinal directions.

The peak of the first harmonic of the flux density in the air gap typically does not exceed the value of 0.9 T [34]. However, because of the retaining sleeve and losses, caused by operation in a high-speed mode, the maximum achievable average flux density is about 0.4 to 0.5 T. Allowable flux density of the tooth and back iron is limited by the saturation of the material, and typically is below 1.5 T. For the exterior rotor, the shell flux density should be less than 1.2 T [30].

Fig. 4.5b illustrates the required sleeve thickness for a given magnet height, while Fig. 4.5a shows the achievable flux density generated by the magnet of the corresponding height. According to the empirical data, a sleeve thickness exceeding 30 mm should not be considered feasible [39]. Consequently, to analyze the plot with dimensionless coefficients, the maximal feasible magnet height requires a sleeve thickness of 30 mm. The flux, which is produced by this maximum magnet height, is correspondingly assumed to be the maximal achievable flux. If Fig. 4.5a was redrawn in terms of comparative dimensionless coefficients, one would see that 90% of the maximum flux density is generated by a magnet with a height that is 35% of the maximum one. In terms of costs it is preferable to have a smaller magnet and thinner sleeve, although the flux density

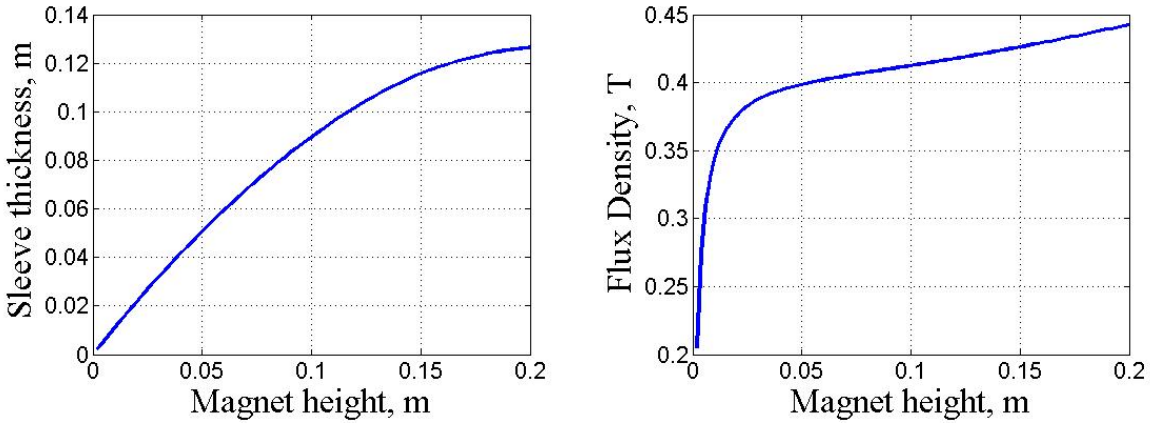

(a) (b)

Figure 4.5: Calculated magnet height versus a) Sleeve thickness b) Flux density. The data is given for 20 MW 10,000 rpm motor design.

will only approximate possible maximum. Thus, the magnet height, which generates 90% of the maximum studied flux is taken as an optimum.

To illustrate the dependence of the optimal magnet height on the rotational speed, Fig. 4.7 should be referred to. The flux density drops with the increase in speed because of corresponding enclosure enlargement (Fig. 4.6b).

4.4.2 Current loading

Thermal calculations. Assuming that the magnetic loading is at the maximal achievable level, current loading defines the maximal shear stress produced by motor. This shear stress level then defines the torque capability of the machine within given limits of rotor volume. The average shear stress of non salient-pole synchronous machines with indirect cooling is in the range of 33.6 to 65.5 kN/m^2 and can have the maximum value up to 148.5 kN/m^2 in direct-water cooled machines [34].

The maximum current loading of the machine is restricted mainly by the temperature considerations. With an insulation of class F, the maximum allowable winding temperature is 130 °C. For specific cooling capabilities, the maximum current loading depends on the slot dimensions. Keeping the ratio of slot width to the slot height as 0.5, winding temperature can be kept below the maximum value when increasing the slot depth. However, according to [40], after 200 mm, further increasing the slot height results in a relative increase in current loading.

Because of the high currents and relatively small sizes, machine thermal capabilities should be carefully studied to avoid damage caused by overheating. A detailed thermal model will be presented in the following sections, however, slot temperature distribution should be known at the stage of the initial sizing to define the slot geometry.

A simplified thermal lumped-parameter circuit can be employed to define the slot size [41, 42]. First crucial assumption is that the hottest spot is located in the top of the

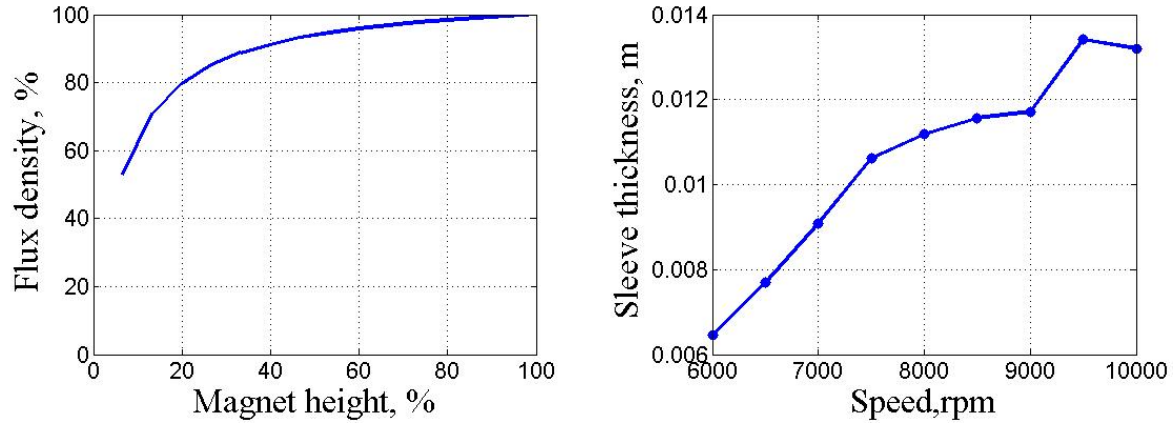

(a) (b)

Figure 4.6: Calculation results of 20 MW PM design: a) Normalized magnet height versus normalized magnet density b) Optimal sleeve thickness versus rotational speed.

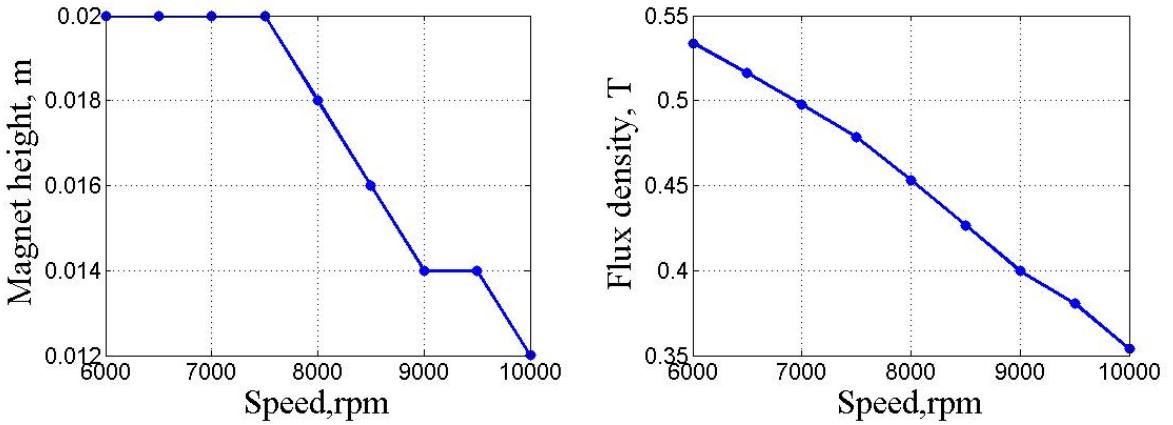

(a) (b)

Figure 4.7: Calculation results of 20 MW PM design: a) Optimal magnet height versus rotational speed b) Normalized flux density versus rotational speed.

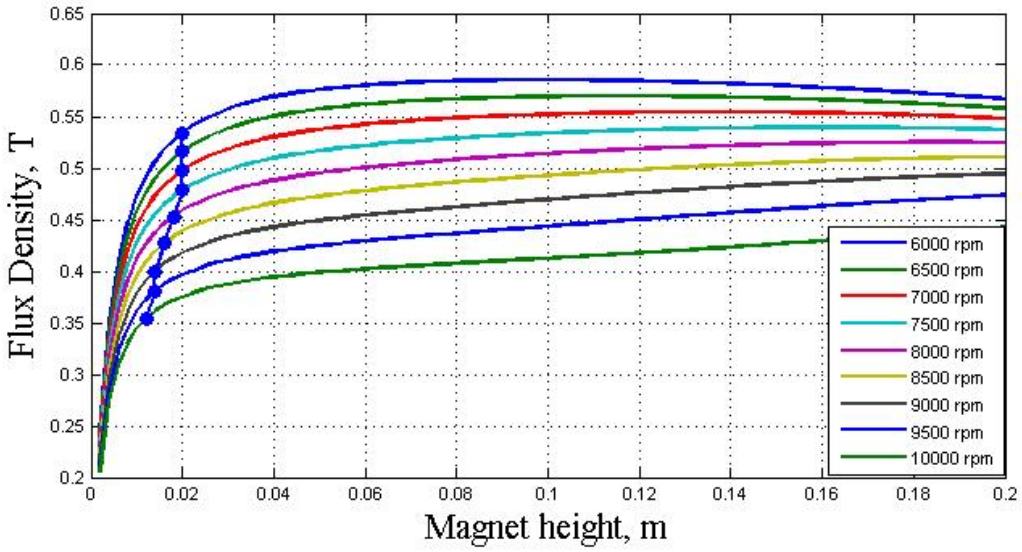

Figure 4.8: Calculated flux density versus magnet height for different rated speed of 20 MW PM motor. Blue line with markers points out optimal flux density. The profile of the line repeats the content of Fig. 4.7a.

slot (to clarify the slot top and bottom location, it is assumed that slot top is located at the same level with the tooth tip and the slot bottom is located near the tooth root). In practice, the hottest spot is located between the slot top and slot center. In slotted high-speed machines there is almost no heat flow from the slot to the air gap, thus, the heat flux passes the tooth and yoke. Because of thin lamination, the axial heat flow is comparatively low and, therefore, can be neglected. Secondly, winding with insulation layers (wire insulation, turn insulation, ground wall insulation, wedge and etc.) is assumed to be homogenous media. Therefore, the average thermal conductivity of the slot is taken between 4 and 7 W/mK [43]. In practice, the winding is highly non-homogenous structure, hence, for the precise thermal calculations, the insulation layout should be known a priori. Now the simple calculations based on the thermal equivalent circuit can be derived.

The thermal resistance of a rectangular bar is governed by the following equation:

$$R_{th} = \frac{l}{\lambda w h} \tag{4.13}$$

Where l,w, and h are length, width and height of the bar. The average temperature change across the resistance is calculated as following:

$$\Theta = \frac{P_{cu}}{R_{th}} \tag{4.14}$$

where P_{cu} represents the copper losses.

Equations (4.13) and (4.14) link slot size and corresponding temperature change. Thus, the maximum buildup of the temperature between the slot wall and its center is sufficient to restrict the slot dimensions.

The equivalent resistance in the thermal circuit is used to model heat transfer between different machine components, such as frame, end-plates, stator and rotor core and so on. Therefore, to determine all the thermal circuit components, it is necessary to know the machine geometry. At the initial stage of machine design, to restrict slot dimensions, it is reasonable to assume that the slot is the only source of heat generation and heat is removed through the slot walls in radial and tangential direction. It is worth noting that slot dimensions, calculated in a such way, will show the minimal slot surface that is necessary to satisfy (4.14).

Number of slots. With a given electrical loading and air gap diameter the number of slots is strictly interconnected with the slot size, which affects the current density. The latter depends on the current and therefore on the number of slots. To make an appropriate selection, an iteration procedure should be applied.

Before calculating current loading, the maximum voltage of the machine should be defined. The voltage is mainly restricted by the capabilities of the converter and the winding insulation. Already mentioned "Perfect Harmony" is able to support voltages up to 12 kV.

Given the maximum back-EMF supported by the converter, the maximum number of turns per phase can be found. Number of slots should be integer and number of conductors in the slot should be even (for a double-layer winding). These constraints severely restrict the domain of feasible solutions. The feasible slot numbers against winding factor are presented in Fig. 4.9.

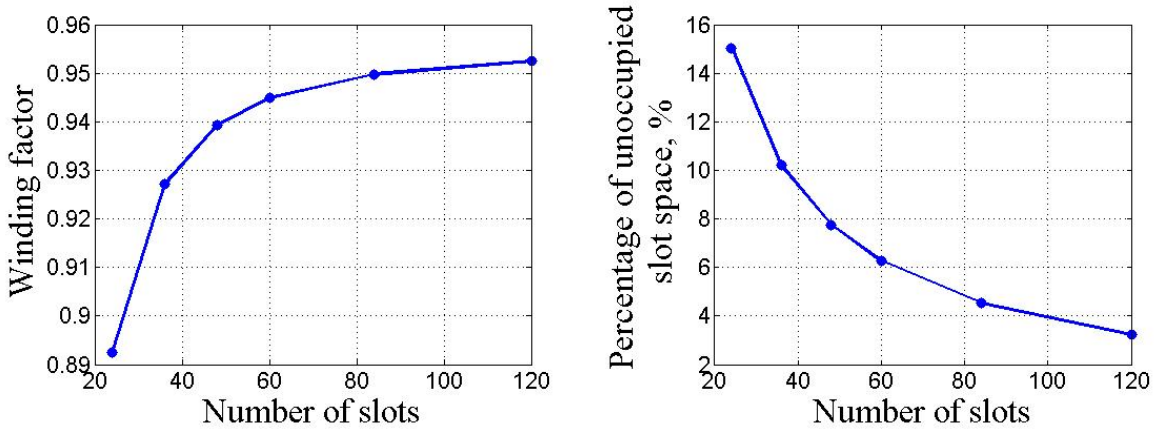

(a) (b)

Figure 4.9: Calculated number of slots: a)Winding factor b)Percentage of unoccupied slot space due to the geometrical restrictions. The data is given for 20 MW PM motor design.

In large machines rectangular slots are used with a nonmetallic wedge. The wedge is used to keep the stator bars tight in the slot and to resist mechanical forces experienced by winding. Dummy slots might be used to decrease the cogging torque. As a slot width, the appropriate height of stator and rotor yokes is selected to avoid flux saturation.

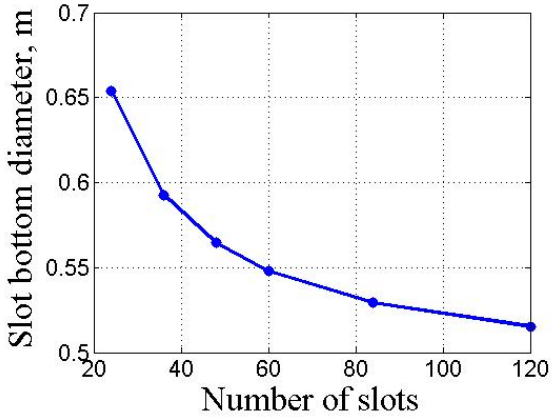

Figure 4.10: Calculated slot bottom diameter versus number of slots. The data is given for 20 MW PM motor design.

Fig. 4.10 illustrates that the slot depth is higher when the number of slots is lower. With a given air gap diameter the number of slots defines the slot width. As a consequence, when the slot width is high, in order to prevent winding overheat, the slot height should be increased to provide sufficient surface for the thermal flow.

4.4.3 Reactance

When the aim of the machine control is to maximize output torque, the synchronous reactance and machine back-EMF will define the required terminal voltage and the reactive power to be supplied from the converter. The converter rating increases as the inverse of the power factor, which means that machine with high reactance will require large and costly electric drive. The power factor of the machine can be increased by the means of control, however, the improvements in power factor in general will inevitably reduce machine shaft power.

The synchronous reactance of the surface magnet three-phase machine is written as follows:

$$X_q = X_d = w_m \cdot p \cdot L_s \tag{4.15}$$

where X_q is q-axis reactance, X_d is d-axis reactance, w is machine mechanical angular speed, p is a number of pole pairs and L_s is synchronous inductance.

Neglecting stator end-winding and slot flux leakages, the synchronous inductance is defined as follows:

$$L_s = L - M$$

where L is a phase self-inductance and M is mutual inductance, which is equal to $\frac{1}{2}L_s$ for a sine-wound machine. L is governed by the following equation:

$$L = \frac{4\mu_0 \tau_p l_s (k_w Q_s)^2}{\pi^2 p \delta_{eff}} \tag{4.16}$$

where τ_p is a pole pitch, l_s is rotor length, k_w is winding factor, Q_s is a number of slots and δ_{eff} is the effective length of the air-gap, which reflects the magnetic reluctance of the machine main magnetic circuit. Therefore, the synchronous inductance and reluctance are lower when the machine effective air-gap is higher.

The high speed of rotation increases machine reactance. At the same time, as was mentioned above, the retaining sleeve increases the effective machine air-gap and, therefore, decreases inductance. In the section above, the optimal sleeve thickness was selected only with consideration of the optimal air-gap flux density. As it follows from (4.16), the obtained inductance can be also taken into account when the sleeve thickness is chosen.

An alternative manner to decrease reactance is to decrease the number of winding turns per phase. Yet, extremely small number of turns per phase (one turn per two slots) will lead to the mechanical complexity, so as it will be difficult to firmly fix a conductor in a slot.

The use of concentrated windings instead of sinusoidally distributed can be another option to decrease inductance. However, because the number of machine pole pairs is low, the selection of feasible slots/poles combinations is severely limited. To implement the concentrated winding on the machine with 2 pole pairs and 48 slots, one would need to use four converters connected in parallel.

The synchronous reactance of the machine plays an important role in the selection of proper electric drive. It should be noted that analytical calculations of the reactance presented above are not enough for an accurate assessment and, therefore, a finite-element modeling should be employed.

4.5 Gear

4.5.1 Assessment of gearbox mass

As was mentioned, typical rotation frequency of the propeller on the heavy vessel is about 150 rpm [9, 14]. Motor operating at the speed of 10,000 rpm will need gearing ratio of 66:1 with output torque of 1,300 kNm to make the drive system feasible. To estimate the mass and feasibility of the gearbox with required characteristics, the careful review of the empirical data and manufacturer's data sheets is necessary.

Epicyclic gearboxes, as illustrated in Fig.4.11, provide high torque density and are suitable for high-power applications. As an example, 12 MW 5,600 rpm three-stage epicyclic gearbox with a ratio of 75:1 has a torque density of 250 kNm/m^3 [45], while the torque density of the motor with a shear stress of 50 kN/m^2 is 100 kN/m^2. Therefore, it can be initially assumed that mass of a combination of a high-speed motor and a gearbox will be lower than mass of low-speed motor alone. On one hand this assumption is valid as long as torque density of the gearbox is much higher than the torque density

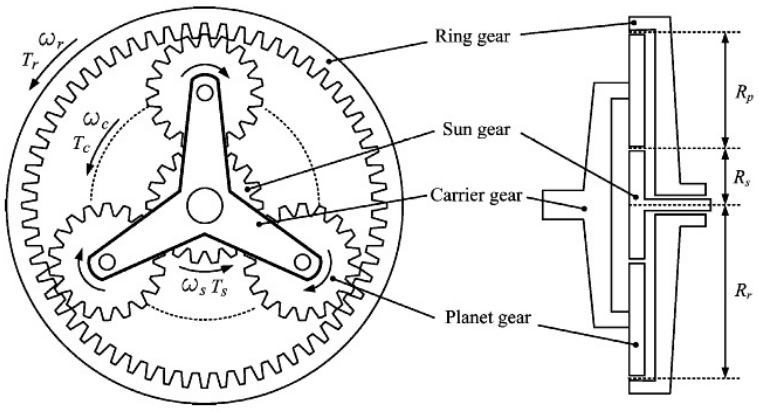

Figure 4.11: Sketch of a typical epicyclic gearbox. ω and T are angular frequency and torque correspondingly, and subscripts p, s, r, c denote planet gear, sun gear, ring gear or carrier arm [44].

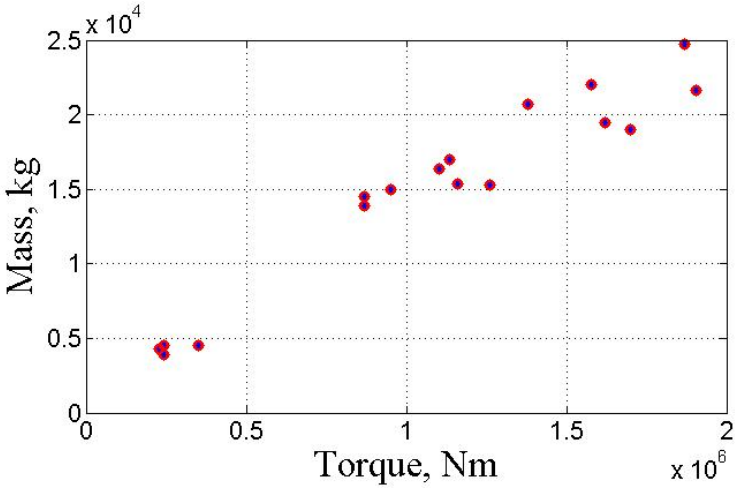

Figure 4.12: Gearbox mass versus input torque. Based on the datasheet of [46].

of the machine. However, the latter should be treated carefully. Generally, shear stress at high speeds becomes lower so as the machine diameter become lower, following the restriction of the maximum surface speed. Therefore, the torque density of the motor drops. If the same is valid for a gear and for a given power, increase of the gear ratio will result in decrease of the torque density, than there should be an optimal speed that will lead to the lowest possible volume of the propulsion system. To get more precise information on what speed the machine should be used to minimize the total mass, a gearbox should be designed. In this respect, this report provides some first order estimates to determine the gearbox mass and volume.

As there is a lack of empirical data on gearboxes for the applications of more than 10 MW, modern wind turbine gearboxes are taken as a reference to estimate the possible mass of the gearbox for 20 MW drive system. The GPV500D model produced by Bosch Rexroth is investigated. The following preliminary assumptions are derived:

1. Gearbox mass depends on the maximum input/output torque (Fig. 4.12). With

a given torque, power rating of the gearbox affects only the speed of rotation of the pinions that should not exceed 250 m/s [45]. Therefore, if this limit is not exceeded, the machine mass will be independent on power in a short range that depends on the gear construction and diameters of the pinions.

2. To compensate the power increase of 20 MW gearbox compared to GPV500D it is assumed that additional stage should be used, which will increase the mass approximately on 1:4. As it follows from Fig. 4.12, the expected mass of a gearbox for 20 MW machine will be approximately 20 tonnes.

3. Typical gear ratio for epicyclical gear is between 1 and 12. However, the amount of teeth influences the pinion diameter and therefore gear ratio affects the mass of the pinions. If it is assumed that the gear ratio is constant in this range, for a three stage gearbox theoretical range of the constant mass is $1:12 \times 1:12 \times 1:12 = 1:1728$. Still, for a combined type of gear mass dependence on the gear ratio should be treated with caution.

4.5.2 Mechanical gearbox design

To design a gearbox a lot of different parameters and factors should be analyzed, such as teeth profiles and its thickness, meshing interference, allowable stresses and bending, and many others. Practical issues of gearbox design process are well described in [47] and the complete theory of machine design is given in [48]. These can be used as guidelines for approximate calculations. It will be shown further that having made a number of assumptions it is possible to estimate geometry and configuration of a gearbox that satisfies the requirements to input torque, speed and gear ratio, presented in Table4.5. The design of GPV500D is chosen as a reference to assist in proper selection when multiple options for certain parameters are available during design process.

To achieve high-torque densities and a high gear ratio, a compound two-stage epicyclic gearbox is used, sketch of which is illustrated in Fig. 4.13. At the initial stage of the design it is complicated to estimate optimal split of gear ratios between two stages. However, keeping in mind that epicyclical gears maximum gear ratio is 1:12, it can be assumed that the first stage would have a ratio of 1:11 and the second stage a ratio of 1:6, thus, in total, providing ratio of 1:66, as required for 20 MW propulsion system.

There are three main configurations of a typical epicyclic gearbox, depending on what gear is fixed and does not rotate. In a chosen configuration a sun gear of the second stage is attached to the arm carrier of a first stage and electrical motor shaft is attached to the sun gear of a first stage. Therefore, the only component that can be fixed in such configuration is a ring gear. The amount of planets does not affect gear kinematics and can be chosen rather freely. Typically, there are 3 to 6 planets in an epicyclic gearbox, however, for specific applications this number can be different. After the gear configuration has been defined, approximate gear geometry can be calculated.

To calculate rotational speed of gears, the tabulation method, described in [47] can be used. For a chosen gearbox configuration, the following relations between sun, carrier, planets and ring gears are valid:

$$\frac{n_s}{n_l} = 1 + \frac{N_a}{N_s} \tag{4.17}$$

$$N_a = N_s + 2N_p \tag{4.18}$$

where n_s and n_l are rotational speeds of sun and carrier, and N_a, N_p and N_s are numbers of teeth of the ring, planet and sun gears, correspondingly.

As it follows from [47], for heavy duty and high-speed applications, the minimum number of gear teeth is 16. However, for the sake of stability and safety, the number of teeth of a sun gear is taken as equal to 20.

To calculate gear geometry, tooth proportions should be known. To characterize geometry of gears independently on the number of teeth, a standard basic rack tooth profile is used, dimensions of which can be found in [49]. With simplified calculations, selection of a standard basic rack ensures proper gear meshing, so as teeth of all gears belonging to a concrete stage will have the same thickness.

For determining the gear pitch circle diameter D (hereinafter is referred to as gear diameter), a power rating equation can be employed [50]:

$$P_{at} = \frac{n_p \cdot DP \cdot K_v}{126000 \cdot K_a} \frac{F}{K_m} \frac{J}{K_s \cdot D} \frac{S_{at} \cdot K_1}{K_r \cdot K_t} \tag{4.19}$$

where n_p is gear rotational speed, DP is gear diametrical pitch, which is equal to the number of teeth per unit of pitch diameter, F is gear facewidth and the rest variables are different factors, description of which is given in [50]. So as designed gearbox is a subject to high load, the facewidth of the gears is taken equal to $1.5D$, which is in the range of typical gear facewidth ($0.5D...2.5D$).

After the number of sun gear teeth is defined, its diameter and length are calculated with (4.19). To determine the geometry of the rest gears belonging to the first stage, a fundamental law of gearing is used [47]. According to the law, surface speeds, defined at the pitch diameter, of two contacting gears are the same, which means that relation of its diameters is inversely proportional to the relation of its angular velocities:

$$\frac{w_1}{w_2} = \frac{D_2}{D1} \tag{4.20}$$

where w_1 and D_1 are angular speed and diameter correspondingly of the driving gear and w_2 and D_2 are angular speed and diameter correspondingly of the driven gear. Substituting N_a from (4.18) into (4.17) and keeping in mind that number of teeth of the sun gear was chosen as equal to 20, the numbers of teeth of planet and ring gears are calculated. The planet gear diameter is calculated from (4.20) and ring gear radius is equal to the sum of a sun gear radius and a planet gear diameter.

To calculate the second stage of a gearbox the same design steps, as described above, are performed. However, it should be kept in mind, that the input speed for the second stage is lower according to the gear ratio of a first stage.

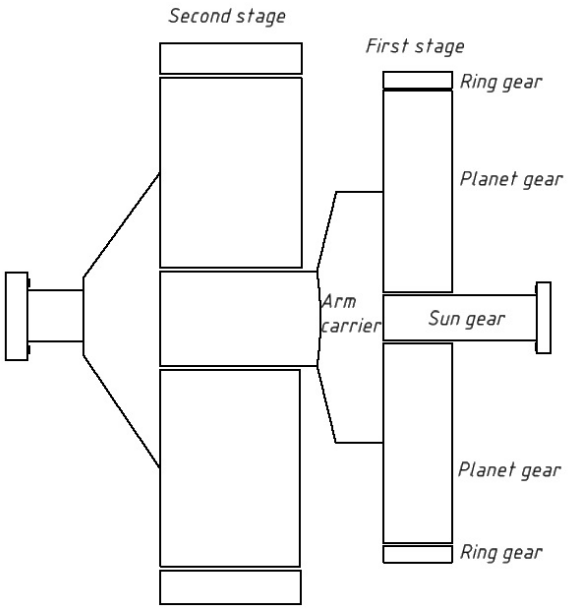

Figure 4.13: Sketch of the two-stage compound 20 MW gearbox with gear ratio 1:66 and input speed of 10,000 rpm.

4.5.3 Magnetic gear

Firstly introduced magnetic gearboxes had a strong visual similarity with the mechanical ones. The crucial difference between magnetic gears and its mechanical analog was that in magnetic gears teeth were replaced by magnets. Such gears had poor torque density, so as only a few of magnets were utilized simultaneously. The concept of a high-performance coaxial magnetic gear, illustrated in Fig.4.14, was proposed by K. Atallah in 2001 [51]. Though magnetic gearbox with a such value of torque density has not been manufactured yet, it was estimated that an optimized magnetic gearbox might have torque density up to 150 kNm/m^3, which is comparable with the torque density of mechanical epicyclic gearboxes.

The mass of a magnetic gearbox has been based on the assumption that the torque density of the gearbox is 100 kNm/m^3. To provide a high gear ratio, gearbox is compound of two stages. Because a high-speed rotor of the first stage have input speed of 10,000 rpm, its diameter is restricted with a maximum surface speed. When the diameter of the internal rotor is defined, its maximum length is calculated with (4.8). The total radial length of the air gap and slot piece is small compared to the rotor diameter, therefore, diameter of the outer rotor can be taken equal to the diameter of the inner rotor, which allows to estimate volume of a first stage of the gearbox. The same logic is applied for calculating the volume of the second stage.

Based on the assumptions and reasoning explained above, in a first-order approximation, the mass of the first stage is calculated as 30 tonnes, mass of the second stage as 10 tonnes, and the total mass of the magnetic gearbox is calculated as 40 tonnes.

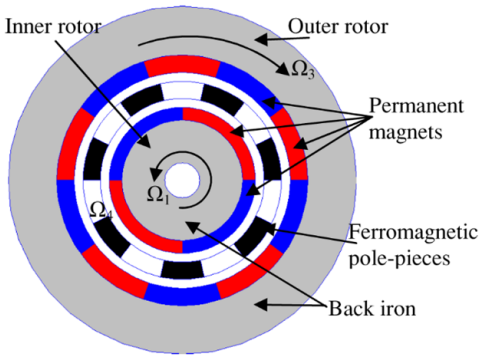

Figure 4.14: Coaxial magnetic gear. Ω is rotational speed of a corresponding gear [52].

Because of complex interaction of magnetic fields in a coaxial magnetic gear, a numerical as well as analytical method that are used for calculations of magnetic field distribution and gear sizing, are time-consuming and require in-depth analysis of the considered electromagnetic processes. Time restrictions prevented inclusion of the magnetic gear calculation to be performed and hence could be a topic for the future work.

4.6 Conclusion

Calculated design of a 20 MW 10,000 rpm PMSM

In this chapter, the main issues of 20 MW high-speed motor design were reviewed and analyzed. The main design trade-offs were presented and investigated, and the recommendations on the selection of suitable solutions were given.

In section 4.4 it was estimated that the rated speed of 20 MW motor can reach 10,000 rpm. The guideline for rotor diameter to length ratio selection was given and it was explained why it is preferable to have a largest possible rotor diameter selected with regard to the rotor critical speed.

It was shown that selection of the optimal magnet thickness and magnet protection (sleeve) calculation are one of the major issues in megawatt high-speed motor design. The carbon sleeve is used to protect magnets from destruction because of huge centrifugal forces, however, the efficiency of magnets usage is inversely proportional to the sleeve thickness. It was explained how the optimal magnet thickness can be calculated and how it depends on the design rated speed.

To define a number of slots, its dimensions and maximal current loading, a thermal model, based on the lumped-parameter equivalent thermal circuit, was employed. In megawatt machines, stator winding consists of rectangular copper bars, which are located in stator slots. For a given rotor diameter, increasing number of slots will lead to the increase in unoccupied slot space, which leads to the decrease in efficiency compared to machines of the same sizes. However, little number of slots negatively influences machine thermal capabilities. In the final design it was calculated that optimal number of slots is 60 for a 20 MW machine.

Tables 4.2, 4.3 and 4.4 contain the calculated data of the proposed optimized machine design with rated power of 20 MW and rated speed of 10,000 rpm.

Calculated design of a mechanical gearbox

In section 4.5 a design of a 20 MW gearbox with a gear ratio of 1:66 was presented. Based on the data for wind turbine gearboxes it was estimated that mass of a such gearbox is about 20 tonnes. The calculated gearbox mass is approximately 25 tonnes that is in a good correspondence with the initial assessment. A guideline for the gearbox design was given, and it was explained how to define dimensions of a mechanical gearbox and number of teeth on different gears. Also a first order estimation of magnetic gearbox mass was given.

Table 4.5 represents gearbox design input parameters, while Table 4.6 contains the calculated data of the proposed mechanical gearbox design.

Parameter	Value	Unit
Number of slots	60	-
Number of poles	4	-
Number of slots per pole per phase	5	-
Number of turns per phase	40	-
Number of conductors in one slot	4	-
Winding factor of the fundamental wave	0.9	-
Winding type	Sine-wound	-
Stack length	1,333	mm
Stator back iron height	47	mm
Tooth tip diameter	500	mm
Rotor outer diameter	445	mm
Sleeve height	7.7	mm
Magnet height	16	mm
Air gap length	3.9	mm
Magnet pole arc	2.5	rad
Slot depth	62.1	mm
Slot width	15.7	mm
Slot fill factor	0.5	-

Table 4.2: Geometry and winding data of 20 MW motor.

Parameter	Value	Unit
Rated power	20,000	kW
Shaft torque	19	kNm
Base speed	10,000	rpm
Air gap shear stress	37	kN/m^2
Back EMF, RMS	9.3	kV
Phase voltage, RMS	22.7	kV
Phase current, RMS	954	A
Phase voltage fundamental frequency	333	Hz
Electric loading	41	kA/m
Current density	2445	kA/m^2
Air gap average flux density at open conditions	0.4	T
Power factor	0.4	-

Table 4.3: Load data of 20 MW motor.

Parameter	Value, kg
PM mass	186
Sleeve mass	26
Copper mass	540
Rotor mass	1532
Stator yoke mass	802
Total teeth mass	429
Total machine mass	3488

Table 4.4: Mass data of 20 MW motor.

Parameter	Value
Input torque, kNm	19
Output torque, kNm	1,270
Input speed, rpm	10,000
Output speed, rpm	151
Gear ratio	1:66

Table 4.5: Gearbox input parameters.

Parameter	Value	
	First stage	Second stage
Type	Epicyclic	Epicyclic
Input torque, kNm	19	210
Input speed, rpm	10,000	909
Output speed, rpm	909	151
Gear ratio	1:11	1:6
Number of planet gears	5	5
Number of teeth, sun gear	20	20
Number of teeth, planet gear	90	40
Number of teeth, ring gear	200	100
Radius of the sun gear, m	0.11	0.23
Radius of the planet gear, m	0.49	0.46
Radius of the ring gear, m	1.1	1.15
Radius of the arm carrier, m	0.6	0.69
Tooth height, m	0.04	0.07
Facewidth, m	0.33	0.69
Total mass, tonnes	12	13

Table 4.6: Gearbox design parameters.

Chapter 5

Down-Scaling Machine Power Rating.

The design of 1 MW or even 100 kW machines is different than the design of 20 MW machine. Mostly affected by the application specific requirements, design solutions also strongly depend on machine rated power. That means that if one would take as a reference machine of 20 MW and design a machine of 1 MW by simple down-scaling of geometrical parameters, it is much likely that obtained solution would not be the optimal one. The reason is that there is no straightforward answer how the design trade-offs are influenced by the machine rated power and speed. Thus, to investigate high-speed machine design for large automotive applications it is important to understand how scaling down the rated power affects geometrical and operational characteristics of the motor.

5.1 Geometry of the machine with less power

Diameter to length ratio As was discussed in 4.4.1, one of the first steps in electrical machine design process is a calculation of rotor geometry. It was explained how the criterion to determine rotor diameter to length ratio can be established for a 20 MW machine. However, if the same criterion is employed for the machine with rated power of 1 MW, and it is assumed that shear stress is 50 kN/m^2 and the maximum surface speed is 250 m/s, calculated rotor length will be less than 0.01 m. Such short rotor is not practical because of high end-winding losses and poor utilization of generated magnetic field. Therefore, maximum surface speed that was used as a reference parameter to define diameter of 20 MW machine, can not be used for the machine, the rated power of which is 100 kW. Apparently, a newly introduced criterion for rotor diameter/length ratio calculation should be employed.

In order to gain insight into the reasoning of rotor diameter/length ratio selection, it is necessary to investigate how machine characteristics, such as efficiency, losses, heat generation and others are varied for different ratios. If only a torque generation of the machine is considered and the shear stress is given as input parameter, produced torque depends only on the rotor volume. Apparently, diameter and length could not be defined if only the rotor volume is given. However, the machine with higher rotor diameter will have excessive end-windings, which do not participate in torque production. Therefore,

such machine will have lower efficiency compared to the machine with lower diameter. From the point of view of thermal capabilities, long diameter is also advantageous as well as disadvantageous depending on the cooling type. In an air-cooled machines the important parameter is the size of the end-winding surface that is in a contact with an ambient. Apparently, large end-windings provide useful path for heat dissipation. At the same time, in water-cooled machines, end-windings generally are the hottest spot of the machine, so as cooling fluid has no common surface with the end-windings. Thus, general conclusion on the heat advantages or disadvantages of having large diameter should be derived with caution.

Machine with very small diameter and long rotor might have not enough space for magnet housing. Moreover, small rotor machine will have deep slots, which is undesirable from the electromagnetics point of view. Thus, efficiency of such a machine might be also compromised. Machines with extremely long rotors should not be selected from the point of view of rigidity.

In applications such as servo-drives, the important issue is matching inertia of the load and the motor. It is desirable to keep rotor inertia low and so as inertia of a cylinder is proportional to the diameter in the power of four, rotor with small diameter is advantageous over the rotor with large diameter. However, in most of the electromotive application it is not possible to match the inertia of the machine and the load and, therefore, such criteria can not be used to define rotor diameter to length ratio.

As it is clear from above, it is necessary to derive a new criterion, which will suit well high power as well as low power machines. For this, the range of investigated machine power should be established. The machine of 20 MW for ship propulsion and machine of 100 kW for electromotive applications can be taken as reference machines, which will limit the maximum and minimum rated power. Inside this range, the machines of 10 MW, 5 MW, 1 MW and 500 kW are investigated. The diameter to length ratio of 20 MW machine is approximately equal to 1/3. In most of electromotive applications, because of practical reasons, electrical machines have a large diameter and a short axial length, therefore, the diameter to length ratio can be taken as equal to one, although that the specific propulsion application should for a final assessment be taken into account. As a result, the diameter to length ratio of the machines, power of which is inside the range of 20 MW to 100 kW will be between 1/3 and 1. A simple linear interpolation can be used to define concrete ratio value. Table 5.1 shows a comparison of geometrical and electromagnetic characteristics between machines with different rated power.

Electromagnetic design The sleeve thickness is one of the parameters which is greatly influenced if the rated power of the machine is 1 MW. Because the rotor is smaller, the centrifugal force, experienced by magnets is less and, therefore, magnet enclosure can be thinner. Apparently, this allows selecting higher rated speed of the motor. Moreover, as was discussed, thinner sleeve allows to achieve higher magnetic flux density. The other advantage of having thin sleeve is that less magnet volume is required to achieve a particular flux density.

To investigate the dependence of a sleeve thickness on the machine rated power, two machines of 20 MW and 1 MW are compared. As it can be seen from Table 5.1, the sleeve thickness of the 1 MW machine is approximately six time less while the

Machine rated power, MW	20	10	5	1	0.5	0.1
Rotor length, m	1.3	0.7	0.5	0.3	0.2	0.1
Stator diameter, m	0.7	0.6	0.6	0.4	0.3	0.2
Diameter to length ratio	0.36	0.68	0.84	0.97	0.99	1
Sleeve thickness, mm	7.7	8.2	5.1	1.3	0.8	0.2
Magnet mass, kg	185	105	55	13	8	2
Optimal flux density, T	0.4	0.4	0.5	0.5	0.5	0.5
Relation of the sleeve reluctance to the total reluctance of the machine main magnetic circuit, %	21.7	20.7	15.8	5.9	3.8	1.2
Rated phase voltage (RMS), kV	9.7	5	2.7	0.8	0.5	0.4
Efficiency, %	94	92	87	84	86	84

Table 5.1: Comparison between machines with different rated power.

total magnet mass is approximately two times lower and the optimal flux density is approximately of the same level. From this comparison it becomes clear that the sleeve thickness does not linearly depend on the machine rated power. It is also worth noting that the relation of the sleeve reluctance to the total reluctance of the machine main magnetic circuit is decreasing with machine rated power increase. Therefore, the air gap flux density of 10,000 rpm machine of 10 MW is less affected by the sleeve compared to the air gap flux density of a 20 MW machine. However, for all presented machines a design trade-off for selection of the optimal flux density is valid, namely, diminishing increase in a flux density with a magnet and rotational speed increase.

As was shown, 20 MW high-speed machines in general will have a low number of turns per coil. However, because of different rotor size, it is possible to have a high number of turns when 1 MW motor is designed. This relative freedom in selection of number of turns is beneficial from voltage and reactance adjustment point of view.

As mentioned, one of the criteria for rated voltage selection was market availability of the high-power converters, which are capable to provide 20 MW power with voltage frequency of 166 Hz. When the machine rated power is down-scaled, the criteria for rated voltage selection might change. It is apparent that an increase in voltage lowers the copper losses for a machine with a given power. However, a high voltage increases the requirements on the winding insulation material and its thickness. That leads to an increase in costs of the machine and a lower packing factor. Therefore, rated voltage

selection can be another design trade-off for 1 MW machine.

To determine rated voltage for a specific rated power, the same reasoning, as it was for selection of diameter/length ratio, can be applied. The rated voltage of 20 MW machine is taken as an upper limit and the lower limit is defined as equal to 690 V line-to-line. The voltage of the machine with the rest rated power will be interpolated.

It is important to keep in mind, that an important input parameter for the motor design is the duty cycle of the propulsion application. A low-speed bulk container requires full power most of the time while a typical city cycle of a vehicle is sharp and the full power is required only during acceleration. When the motor is used in a full-power mode relatively rare from the point of view of operational profile,the motor can be designed in such a way to provide a peak power only in overload mode. Practically, in an overload mode electrical motors can operate at double rated power for a short time, albeit that the overload capability mainly depends on the thermal capabilities.

5.2 Conclusion

This chapter describes the differences between design challenges of machines with different rated power. It was shown how the design trade-offs are influenced by the machine rated power and speed, and how the geometrical data deviates for different machine designs.

A criterion for the selection of diameter to length ratio for different machine rated power was described and machines with rated power from 20 MW till 100 kW were analyzed. It was calculated that for the same rotational speed, machine of less power needs thinner magnet enclosure. The relation of the magnet enclosure reluctance to the total reluctance of the machine main magnetic circuit is less for the machines of less power and, therefore, magnet enclosure design is not critical for the low-power machines.

To compare a design of 20 MW machine with 100 kW machine, one should refer to Tables 5.2, 5.3 and 5.4, which represent data calculated for the proposed design of 100 kW machine.

Parameter	Value	Unit
Number of slots	24	-
Number of poles	4	-
Number of slots per pole per phase	2	-
Number of turns per phase	56	-
Number of conductors in one slot	14	-
Winding factor of the fundamental wave	0.9	-
Winding type	Sine-wound	-
Stack length	115	mm
Stator back iron height	16.1	mm
Tooth tip diameter	117	mm
Rotor outer diameter	95	mm
Sleeve height	0.2	mm
Magnet height	10	mm
Air gap length	0.8	mm
Magnet pole arc	2.5	rad
Slot depth	29.2	mm
Slot width	14.5	mm
Slot fill factor	0.5	-

Table 5.2: Geometry and winding data of 100 kW motor.

Parameter	Value	Unit
Output power	100	kW
Shaft torque	95	Nm
Base speed	10,000	rpm
Air gap shear stress	39	kN/m^2
Back EMF, RMS	358	V
Phase voltage, RMS	2042	V
Phase current, RMS	137	A
Phase voltage fundamental frequency	333	Hz
Electric loading	37	kA/m
Current density	8713	kA/m^2
Air gap average flux density at open conditions	0.5	T
Power factor	0.17	-

Table 5.3: Load data of 100 kW motor.

Parameter	Value, kg
PM mass	2.3
Sleeve mass	0.01
Copper mass	0.6
Rotor mass	6.0
Stator yoke mass	7.9
Total teeth mass	0.6
Total machine mass	17.4

Table 5.4: Mass data of 100 kW motor.

Chapter 6

Application of High-Speed Motors on Vessels

In the previous chapters the benefits of electrical motors as drives were described and analyzed. The main challenges of a high-speed permanent magnet motor design were presented and investigated. However, the important topic, which has not been covered yet by this report, is what configuration of a vessel drivetrain employs better advantages of a high-speed electrical motor. In this chapter, efficiency and implementation of a high-speed electrical propulsion on vessels are investigated.

6.1 Propeller basics

Up to date, screw propeller is the most commonly used type of propulsor. Although a lot of different types of unconventional propulsors are under research for more than decades, for most of the applications propellers still have no competitors [53, 54]. Seeming simplicity of a propeller as a mechanical device may allow one to conclude that it is a trivial task to estimate efficiency of a different propeller arrangement. This conclusion is misleading, so as propeller design requires accurate assessment of the ambient fluid behavior, which is much dependent on the vessel hull shape. Thus, in general, propellers are designed specifically for a particular vessel.

Though a propeller design requires knowledge in naval technology and fluid dynamics, there are a few basic principles which should be mentioned. The highest efficiency of the propeller operation is reached when it is located behind the hull. When ship moves, it drags water around the hull in the direction of its movement. Velocity of the water on the hull surface is almost equal to the ship speed while it becomes zero at a certain distance from the hull. As a consequence, velocity of the wake at a propeller surface is non-zero and depends on the hull shape and propeller location. The kinematic energy, transmitted by the hull to the wake is extracted by the propeller, which stipulates its location in the vessel stern.

In general, distribution of the water velocity along propeller surface is non-homogenous, which increases the risk of propeller cavitation. Cavitation is highly undesirable effect, which causes vibration and propeller destruction. Different mechanical means, such as

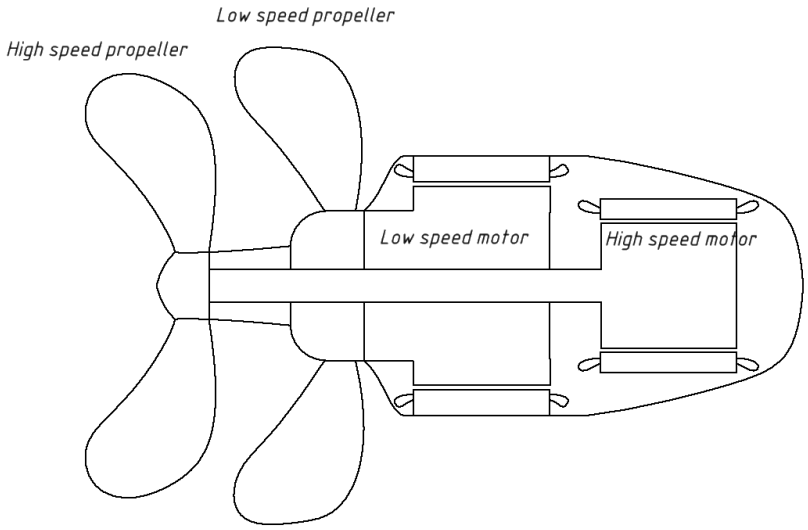

Figure 6.1: POD configuration with two propellers, rotating at different speeds. It is worth noting, that sizes of the motors, which drive propellers are also different according to the rated speeds.

nozzles, ducts and fins are used to make water flow more homogenous. However, the effect of these components is not always positive and should be investigated in details specifically for the ship where it is going to be installed.

The vessel hull shape is designed in such a way to keep the ship's resistance as low as possible. To decrease the wave resistance, the upper water part has a sharp shape with clearly visible wave breaking line. To decrease wave generation, different types of bulbs are applied, while to decrease the drag resistance of the underwater part, the hull profile is made smooth and without any abrupt geometrical elements. The latter is also valid for the propulsors and it is a reason why PODs have a streamlined shape.

To extract most of the energy, contained in a vessel wake, a configuration of a POD with double propeller can be employed (Fig. 6.1). In such configuration, a low-speed propeller accelerates the water stream, thus increasing operational efficiency of a high-speed propeller.

As was mentioned, the power required to propel ship and the propeller rotational speed much dependent on the vessel hull shape. However, it is clear that propeller rotational speed also depends on the required vessel speed. It is also apparent that propeller rotational speed is much different if to compare heavy low-speed cargo carriers and racing boat. Though recently introduced concepts, such as fast ferry, might be a topic of economic studies in further, most of modern heavy vessels are low-speed (Table 6.1). So as it is a strong dependence of propeller speed on the vessel speed, it is clear that high-speed electrical motors that drive propellers directly would be mostly demanded only on high-speed vessels. For low-speed vessels electrically propelled drivetrain should include gearbox to match the propeller speed with the motor speed.

Vessel type	Top speeds
Bulk carriers	16
LNG tankers	25
Fast displacement ships	25
Passenger vessels	30
Navy	40
High-speed crafts	>60

Table 6.1: Typical top speeds of different types of vessels [53].

6.2 Supercavitating propellers

Propeller maximum rotational speed is limited by the cavitation effect. Cavitation is a subject of the numerous studies which have been carrying out since second half of the 20th century. Cavitation occurs in any situation where fluid moves near the solid surface [55]. Because of local high fluid velocities, local pressure of liquid portions becomes low enough for the fluid to change its state [53, 55]. As a consequence, cavitation bubbles, filled with vapor, appear. When there is a rather high amount of bubbles appearing at a small distance near each other, they start to interact and will form cloud cavitation. After cavitation bubbles arrive to the area with high pressure, they collapse. Because bubble collapses asymmetrically, a microjet inflow appears on its one internal side. This microjet reaches very high velocities and its impact on the opposite side of a bubble generates a shock wave which is transmitted to the solid surface [55], producing noise and material erosion.

Cavitation is unavoidable effect which occurs at any speed of propeller rotation. However, when the speed is higher, the damage, caused by cavitation to the propeller blades is stronger. There were attempts to design non-cavitating propeller by varying its geometry, however, these attempts did not show positive results [56]. The other approach to decrease cavitation negative influence was design of a propeller, which operates in the regime of a supercavitation (SC). In such a regime, the cavities collapse behind the blade surface, causing much less damage to the propeller. During 60-80s a few high-speed hydrofoil crafts with SC propellers were manufactured and commercially used. As it is dated by [56], the latest of the hydrofoil ships showed insufficient reliability of the shaft sealing. This disadvantage of the SC propellers appeared to be a crucial one and the further open ocean hydrofoil ships were equipped with water jets.

However, despite the clear end of the SC propellers era in the mid of 80s, there are further modifications, namely surface-piercing, transcavitating propellers and ventilated water jets are to date subjects of ongoing research. Fig. 6.2 illustrates the interdepen-

dence between craft speed, its displacement and type of installed propeller. Apparently, high-speed vessels which employ surface-piercing propellers probably are the most attractive market candidates for electrical high-speed direct-driven drivetrains.

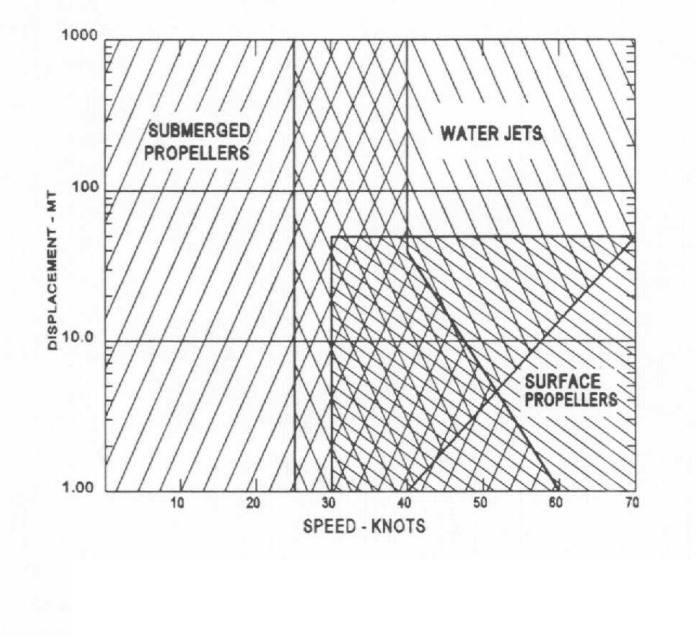

Figure 6.2: Interdependence between craft speed, propeller speed and craft displacement [57].

6.3 Water jet

The other type of drivetrain, which employs high-speed propulsor is a water jet. A water jet comprises a pump, which sucks fluid at the inlet and generates a jet at the outlet. A high-speed jet accelerates vessel. Because pump jets are much more efficient at the high speeds, they are mainly employed on high-speed crafts.

Ones of the largest world manufacturers of water pump jets are Wartsilla and Rolls-Royce. According to the published data, the power of the largest installed Wartsilla jets reaches 20 MW and water jets up to 50 MW available by request. The crucial component of the water jet, which creates the pressure difference between the inlet and the outlet, finally resulting in the jet acceleration, is an impeller. An impeller is installed inside a diffusor, which is fundamentally a pipe at the intake side with an open end (Fig. 6.3). In conventional systems impeller is driven directly by diesel engine or gas turbines via shaft, which is located partly in diffusor, creating an obstacle for the water flow. Such location of the diffusor causes cavitation and increases level of non-homogeneity of the intake water flow. Therefore, removing the shaft might gain efficiency of a water jet propulsion systems.

Generally, the water jet sizing requires data about the hull resistance, demanded thrust and vessel speed. According to Wartsilla datasheet, the speed of impeller rotation lies in the range of several hundred's till several thousand's rpm. Based on the mentioned

Figure 6.3: X-ray view of a water jet, produced by Wartsilla [58].

above, it is likely that high-speed electrical motors with internal impeller can be efficiently used in water jets. Such configuration will not require a shaft and can benefit from the earlier discussed advantages, brought by high-speed motor. A sketch of such configuration is represented in Fig. 6.4

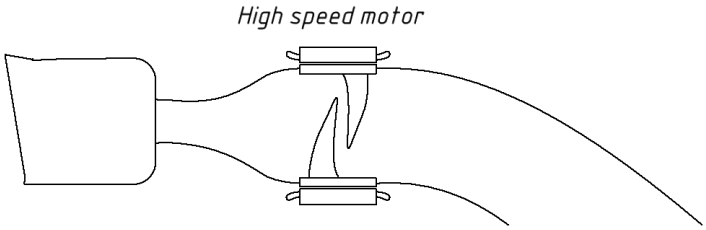

Figure 6.4: Sketch of a water jet with direct-drive high-speed electrical motor.

The other possible type of propulsor is a water track, illustrated in Fig. 6.5. The main advantage of a water track is a constant thrust in forward direction, which is achieved by adjusting blade position. Contrary to conventional propellers, which normally create certain lift in upward direction, operation of water track can be more efficient.

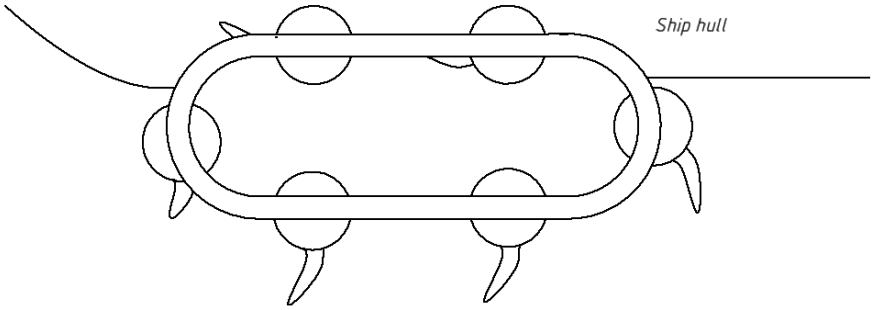

Figure 6.5: Sketch of a water track.

Chapter 7

Conclusions and Future Work

The main driving factors for marine propulsion units are low mass and volume, low noise and vibration, and reliability. With these performance drivers in mind, multi-parametric scans of the salient geometric parameters, gear ratios and pole numbers have been initiated in this first part of the concept study using advanced computational tools. This is supported in turn by empirical data from detailed knowledge about non-linear mechanics, electromagnetics, thermodynamics, etc. that has been acquired with by years of electric drive experience. Further, the combination of modern power electronics with these high-speed propulsion machines offers a huge advantage for propulsion in being compact and providing for an efficient structure. This is enabled by the recent advances in IGBT power switching devices that allow for higher system voltages and hence minimization of interconnection cable mass on the ship.

Further, the obtained results show that in spite of challenges, posed by rotational speed and large power, 20 MW high-speed permanent magnet synchronous motor is feasible and offers the required compactness and efficiency. To calculate a motor design, an algorithm was developed and implemented in Matlab. Calculation results showed that estimated rotor mass is less than 1.5 tonnes and the total machine mass is less than 5 tonnes. That satisfies the initial project requirements to the machine compactness. The maximal speed which can be reached by 20 MW PMSM is estimated as 10,000 rpm. To restrain high centrifugal force experienced by magnets, a carbon sleeve is calculated as 5 to 10 mm. The optimum flux density of the designed motor is around 0.45 T and the shear stress about 50 kN/m^2. The most important characteristics of the proposed motor design are presented in Tables 4.2, 4.3 and 4.4.

In a first-order approximation, the mass of a 20 MW mechanical gearbox with input speed of 10,000 rpm and gear ratio of 1:66 is calculated as 25 tonnes while the total mass of the magnetic gearbox with the same characteristics is calculated as 40 tonnes. Therefore, mass of the combination of the high-speed motor and gearbox is expected to be less than 30 tonnes when mechanical gearbox is employed, and less than 40 tonnes when magnetic gearbox is used. For comparison, the mass of the propulsion module of Azipod XO2100, produced by ABB, is 170 tonnes for output power of 18 MW [23].

The most prospective use of directly-connected high-speed motor for marine propulsion is to employ the motor in a water jet drivetrain. Replacement of a shaft-driven impeller with a high-speed electrical machine might gain increase in the hydrodynamic efficiency

and fuel savings of the propulsion unit. Initially it was assumed that such solution might be patented. However, after the report was submitted to the customer, it was found that a solution for a water jet, which is very similar to the proposed in this report, had already been patented before. Nevertheless, the rest of the proposed configurations can be used for further in-depth research on this topic.

To perform detailed analysis of the proposed in this project motor design and drivetrain configuration, additional multi-disciplinary studies are required in future. Although it is estimated that an application of a high-speed motor will greatly contribute to the compactness and efficiency of modern marine propulsors, only simulations of the complete ship power system and drivetrain will provide a definite answer about the advantages of high-speed PMSM use. After more detailed research on such topics as selection of prime movers, power electronics and control system design, assessment of hydrodynamic efficiency, a prototype of a high-speed motor can be built for performing measurements. If the measured results correspond to the simulations, a propulsor model testing in basin should be performed.

The enormous technological potential of this conceptual high-speed electrical propulsion system, due to high power density of both power electronics and electrical motor, will provide a cost-effective electrical drive system for future marine applications. Although this report only scratched the surface of the required multi-disciplinary research, it supports this statement.

It is expected that the results of the performed work will be further published.

Bibliography

[1] *Reference list LNG carriers electric power and propulsion systems*, ABB AS Marine and Turbocharging, 2010.

[2] "Abb wins 18 million order for subsea pipeline construction vessels," Available: http://www.abb.com/cawp/seitp202/6cbd0102e403ad1285257a0000524030.aspx, 2012.

[3] "Samsung chooses stadt no-loss electric propulsion," Available: http://www.stadt.no/pdf/STADT_SAMSUNG%20ENGLISH%20PR%20REV2.pdf, 2011.

[4] C. Bailey, D. Saban, and P. Guedes-Pinto, "Design of high-speed direct-connected permanent-magnet motors and generators for the petrochemical industry," *Industry Applications, IEEE Transactions on*, vol. 45, no. 3, pp. 1159–1165, May-June 2009.

[5] M. Bogomolov, C. Kral, A. Haumer, and E. Lomonova, "Modeling of permanent magnet synchronous machine with fractional slot windings," in *IECON 2012 - 38th Annual Conference on IEEE Industrial Electronics Society*, Oct. 2012, pp. 1894–1899.

[6] C. Kral, A. Haumer, M. Bogomolov, and E. Lomonova, "Harmonic wave model of a permanent magnet synchronous machine for modeling partial demagnetization under short circuit conditions," in *Electrical Machines (ICEM), 2012 XXth International Conference on*, Sept. 2012, pp. 295–301.

[7] http://www.autodesk.nl.

[8] *Diesel-electric drives*, MAN, Copenhagen, Denmark.

[9] M. R. Patel, *Shipboard propulsion, power electronics, and ocean energy*. CRC Press, 2012.

[10] B. A. Bassham, "An evaluation of electric motors for ship propulsion," Ph.D. dissertation, Naval Postgraduate School, Monterey, California, 2003.

[11] I. R. J. King, *Marine propulsion: the transport technology for the 21st century?*, Rolls-Royce.

[12] *ABB marine catalogue*, ABB Oy Marine, 2008.

[13] *Wartsila ship product catalogue*, Wartsila, 2011.

[14] *Basic principles of ship propulsion*, MAN Diesel and Turbo, Copenhagen, Denmark.

[15] A. K. Adnanes, *Maritime electrical installations and diesel electric propulsion*, ABB AS Marine, Oslo, Norway, 2003.

[16] *SFOC optimization methods*, MAN Diesel and Turbo, Copenhagen, Denmark, 2012.

[17] *Marine engine*, MAN Diesel, Germany, 2009.

[18] *Marine solutions*, Wartsila, Helsinki, Finland, 2012.

[19] "Converteam to supply propulsion systems for u.s. navy's mobile landing platform program," Available: http://www.converteam.com/majic/pageServer/12040001bb0000/en/20110803-US-Navy-Mobile-Landing-Platform.html, 2003.

[20] *Electric propulsion: shipping forecast.* Centaur Communications Ltd, June 2007.

[21] S. Aksu, S. Aksu, and O. Turan, "Reliability and availability of pod propulsion systems," *Quality and Reliability Engineering International*, vol. 22, pp. 41–58, 2006.

[22] http://www.nauticexpo.com.

[23] *Azipod XO2100 Product Introduction*, ABB Oy, Marine, Helsinki, Finland, 2009.

[24] C. Lewis, "The advanced induction motor," in *Power Engineering Society Summer Meeting, 2002 IEEE*, vol. 1, July 2002, pp. 250–253.

[25] R. Lateb, N. Takorabet, F. Meibody-Tabar, A. Mirzaian, J. Enon, and A. Sarribouette, "Performances comparison of induction motors and surface mounted pm motor for pod marine propulsion," in *Industry Applications Conference, 2005. Fourtieth IAS Annual Meeting. Conference Record of the 2005*, vol. 2, Oct. 2005, pp. 1342–1349.

[26] S. Kalsi, K. Weeber, H. Takesue, C. Lewis, H.-W. Neumueller, and R. Blaugher, "Development status of rotating machines employing superconducting field windings," *Proceedings of the IEEE*, vol. 92, no. 10, pp. 1688–1704, Oct. 2004.

[27] http://www.ae-magnetics.nl.

[28] K. Kullinger, *High-megawatt electric drive motors*, ABB BU Machines, 2009.

[29] A. Borisavljevic, H. Polinder, and J. Ferreira, "On the speed limits of permanent-magnet machines," *Industrial Electronics, IEEE Transactions on*, vol. 57, no. 1, pp. 220–227, Jan. 2010.

[30] J. Hendershot and T. Miller, *Design of brushless permanent-magnet machines.*

[31] K. G. Kerszenbaum, I., *Operation and maintenance of large turbo-generators.* Wiley-IEEE Press, 2004.

[32] Z. Kolondzovski, A. Arkkio, J. Larjola, and P. Sallinen, "Power limits of high-speed permanent-magnet electrical machines for compressor applications," *Energy Conversion, IEEE Transactions on*, vol. 26, no. 1, pp. 73–82, Mar. 2011.

[33] K. Binns and D. Shimmin, "Relationship between rated torque and size of permanent magnet machines," *Electric Power Applications, IEE Proceedings* -, vol. 143, no. 6, pp. 417–422, Nov. 1996.

[34] J. Pyrhönen, T. Jokinen, and V. Hrabovcová, *Design of rotating electrical machines.* Wiley, 2008.

[35] K. Weeber, *Advanced electric machines technology*, GE Global Research, 2009.

[36] J. Bone, "Influence of rotor diameter and length on the rating of induction motors," *Electric Power Applications, IEE Journal on*, vol. 1, no. 1, pp. 2–6, Febr. 1978.

[37] *ROBICON perfect harmony - the leading medium-voltage drive*, Siemens AG Industry Sector, 2009.

[38] G. Slemon, "On the design of high-performance surface-mounted pm motors," *Industry Applications, IEEE Transactions on*, vol. 30, no. 1, pp. 134–140, Jan.-Febr. 1994.

[39] Private interview with Dr. F.J.M. Thoolen at CCM, June 2013.

[40] A. Grauers and P. Kasinathan, "Force density limits in low-speed pm machines due to temperature and reactance," *Energy Conversion, IEEE Transactions on*, vol. 19, no. 3, pp. 518–525, Sept. 2004.

[41] A. Boglietti, A. Cavagnino, and D. Staton, "Determination of critical parameters in electrical machine thermal models," *Industry Applications, IEEE Transactions on*, vol. 44, no. 4, pp. 1150–1159, July-Aug. 2008.

[42] P. Mellor, D. Roberts, and D. Turner, "Lumped parameter thermal model for electrical machines of tefc design," *Electric Power Applications, IEE Proceedings B*, vol. 138, no. 5, pp. 205–218, Sept. 1991.

[43] J. Paulides, "High performance 1.5mw 20,000rpm permanent-magnet generator with uncontrolled rectifier for 'more-electric' ship," Ph.D. dissertation, Department of Electronic and Electrical Engineering, University of Sheffield, Sheffield, United Kingdom, 2005.

[44] J. Linni, "Design, analysis and application of coaxial magnetic gears," Ph.D. dissertation, Department of Electrical and Electronic Engineering, The University of Hong Kong, Pokfulam, Hong Kong, 2010.

[45] D. Hofmann, "Gearing for high speed motors," in *High Speed Bearings for Electrical Machines (Digest No: 1997/164), IEE Colloquium on*, Apr. 1997, pp. 301–313.

[46] *Gearbox technical information GPV 500D*, Rexroth Bosch Group.

[47] G. Maitra, *Handbook of gear design.* Tata McGraw-Hill, 1994.

[48] J. Shigley, C. Mischke, and T. Brown, *Standard handbook of machine design*, ser. McGraw-Hill Standard Handbooks. McGraw-Hill, 2004.

[49] H. Merritt, *Gear engineering*, ser. A Halsted Pr. Book. Wiley, 1971.

[50] P. Lynwander, *Gear drive systems: design and application*, ser. Dekker Mechanical Engineering Series. Marcel Dekker, 1983.

[51] K. Atallah and D. Howe, "A novel high-performance magnetic gear," *Magnetics, IEEE Transactions on*, vol. 37, no. 4, pp. 2844–2846, Jul. 2001.

[52] E. Gouda, S. Mezani, L. Baghli, and A. Rezzoug, "Comparative study between mechanical and magnetic planetary gears," *Magnetics, IEEE Transactions on*, vol. 47, no. 2, pp. 439–450, Feb. 2011.

[53] G. Kuiper, *Lectures: resistance and propulsion*, Technical University Delft, the Netherlands.

[54] Private interview with prof. Dr. ir. van Terwisga at MARIN, Oct. 2013.

[55] P. Randall W. Whitesides, *Interesting facts (and myths) about cavitation*, PDH Center.

[56] A. Achkinadze, *Supercavitating propellers*, Saint-Petersburg State Marine Technical University, Russia.

[57] B. R. Blount, D.L., "Design of propulsion systems for high-speed craft," *Marine Technology and SNAME News*, vol. 34, no. 4, pp. 276–292, 1997.

[58] *Wartsila propulsors*, Wartsila, Helsinki, Finland, 2011.

Appendix A

Baseline Document

Review-versions

Due to the unforeseen reasons, which are out of the scope of this report, the project management of this project was done after the actual finalization of the project. However, the project management document was under development for more than one month and, therefore, the final version was greatly improved compared to the initial one. Through a number of revisions some modifications were made. The most important ones are:

1. *Introduction:* was modified to focus on the description of the project "background" and give better clarity to those not acquainted with the topic.
2. *The project result:* definition, results and delimiters were modified for a few times for the sake of clarity.
3. *Activities in each project phase:* strategy was introduced, which led to smoother adaption of the tasks. The separation of the tasks is now better distributed in each phase.
4. *Control plan:* time assignment for each phase and task varied significantly throughout the project and the revision of this report. Gantt chart with margins was added. Information about budgets and spending were acquired. Quality control was extended with more explicit details.

1. Introduction

Electrical propulsion in the marine sector is an emerging technology which has been under development since the beginning of the last century. Though nowadays electrical propulsion is considered a standard for cruise ships and is ever more implemented on icebreakers, service vessels (aeronautic, research, pipe-laying) and offshore drilling platforms, it is still a challenging area, which stimulates research of more efficient electric drives and different drivetrain configurations which can be applied in different marine applications.

Customer is a research and development company, which is mainly focused on the development of intellectual property, testing and certification of diverse electric apparatuses. The company is actively being searching for disruptive electrical technologies in different areas. Though large part of customer's business is connected with the automotive electrical applications, the company is also interested in the development of new types of marine electrical propulsors, which can bring significant benefits for the ship owners. Proposed by the assistant professor from Electromechanics and Power Electronics Group, Dr. Johan Paulides, a new concept for electrical ship propulsion, which employs high-speed permanent magnet synchronous machine (PMSM), was accepted by the customer and became a main topic of this project.

The aim of this project is to give a general introduction to the concept of electrically-propelled vessels and present a feasibility study of 20 MW high-speed PMSM to be used for ship propulsion. This project is executed as the final project of the Professional Doctorate in Engineering (PDEng) in Information and Communication Technology, a two years program that is offered by the Stan Ackermans Institute (SAI) at TU/e. The supervisors of the project are Dr. Johan Paulides and Dr. Alexandar Borisavljevic from the EPE Group, TU/e.

2. The project result

2.1. Problem definition

The demand for compact and efficient electrical drives has created an opportunity for high-speed permanent magnet synchronous motors (PMSM) use for ship propulsion. In order to assess a feasibility of a chosen concept, one may need to investigate power limits of high-speed machines, design challenges and possible solutions. Therefore, the present project is focused on investigation of 20 megawatt (MW) electric drive, where the system constraints for marine propulsion will be considered. The outcome of the project will constitute a concept study and not an in-depth system analysis that would be required when implementing this technology for an electrical drive in future ships.

2.2. Results

The expected result of the project is a feasibility study of a high-speed high-power electrical motor for ship propulsion. Thus, the main outcome is:

- Report.
- Presentation.

2.3. Deliverables

The final report should include the following topics:

- Analysis of potential benefit brought by implementation of electrical propulsion on vessel.

- The conceptual design of high-speed electrical motor and its major operational and geometrical characteristics.
- The comparison between high-speed motors with different rated power.
- Gearbox assessment and approximate calculation.
- The overview of possible drivetrain layouts which employ high-speed electrical motors.
- Proposal for new types of propulsors and short description of the advantages brought by the proposed configuration.

2.4. Delimiters

- The outcome report will constitute only a concept design. In this respect, only the main challenges of high-speed high-power machine will be investigated, which means that the calculated motor parameters should be used only as guidelines for further, in-depth research.
- The thermal behavior of the motor is out of consideration.
- The hydrodynamics of the possible propulsors with high-speed electrical motors is not investigated.
- Propeller design and ship's wake modeling are not investigated.

3. Project activities

3.1. Strategy

Depending on the goal and deliverable results project can be divided in different phases. Apparently when the main outcome of a project is a product of any type and the project starts from "scratch", all the activities performed during the project can be divided into six phases, namely initial, definition, design, preparation, realization and follow-up phase. However, the main goal of the current project is a feasibility study and conceptual design, therefore, the project itself can be considered as a design phase of some larger project. The other way to divide current project into phases is to think about the main goal, as about a process, which has six mentioned phases. However, because such an approach will inevitably bring complexity and vagueness in defining activities that should be performed in each phase, the following strategy was used. As was mentioned, the final report is the main outcome of the study. The first, second and third chapters of the final report introduce the concept of electrical propulsion on ships and define main challenges of the high-speed machine implementation. Therefore, from the point of view of project management, these chapters describes the activities performed during the definition phase. The fourth and fifth chapters investigate the challenges of a 20 MW motor design and possible solutions. In this respect, the content of these chapters correspond to the design phase of the project. The sixth chapter contains information

relevant for the realization phase of the project, namely implementation of the high-speed motors on ships and possible configurations of propulsors. A preparation and follow-up phases are skipped because of absence of the corresponding activities.

3.2. Initiation phase

Activities:

- Compose technical proposal.
- Define desired results and requirements.

End:

- Project assignment.

3.3. Definition phase

Activities:

- Discuss with supervisors possibilities of application of high-speed permanent magnet motors on vessel.
- Share experience and review the work which was done by supervisors in similar areas.
- Define the requirements to the drive systems of large vessels.
- Define what types of propulsors are investigated.
- Explore the benefits and drawbacks of electrical propulsion on ships.
- Review modern types of vessel propulsion.
- Identify challenges of future propulsion systems.
- Estimate benefits of electrical propulsion on vessels.
- Make an overview of types of electrical motors which are used for ship propulsion.
- Make an overview of 20 MW high-speed motor design challenges.
- Define rated rotational speed and power of investigated motor.

End:

- Chapters 1, 2 and 3 of the final report.

3.4. Design phase

Activities:

- Comprehensive analysis of datasheets issued by the main manufacturers of electrical motors and diesel engines for the marine industry.
- Calculation of magnetic and electric loading.
- Selection of rotor to length ratio for 20 MW high-speed permanent magnet motor.
- Calculation of rotor sleeve thickness.
- Selection of optimal magnet thickness.
- Determining number of slots of a motor.
- Modeling of thermal behavior of the motor.
- Calculation of gearbox dimensions.
- Comparison of calculated motor parameters for different power ratings.

End:

- Chapters 4 and 5 of the final report.

3.5. Realization phase

Activities:

- Determination of new conceptual propulsor's configurations.

End:

- Chapter 6 of the final report.

4. Control plan

4.1. Time

4.1.1 Control of progress

- Short weekly meetings with supervisor in TU/e.

Title	Date
Starting date of the project	01.04.2012
Completing date of the project	30.11.2012
Initial phase duration	1 week
Definition phase duration	2 months 3 weeks
Design phase duration	6 months
Delivery date for the results	30.11.12
Final presentation	To be determined
Project participant	**Man hours**
Capacity – Maxim Bogomolov	40 hours/week
Capacity - TU/e supervisor	10 hours/month

Table A.1: Overview of time/capacity.

- In the Gantt chart, presented in the end of the document, the timeline of the project is shown. Three vertical red lines indicate important deadlines – submitting of the preliminary report, submitting of the final report and submitting of the improved version of the final report, according to the remarks, obtained from the customer. August, 24th was agreed as a date of preliminary report submitting. The preliminary report should consist of not less than 20 pages and contain information about performed work at the moment of submitting. November 30th is the date when final report was submitted and the hard copy of the improved version of the final report was send to the customer on December, 20th.
- Approximately one presentation per 3 weeks was prepared. The first presentation for customer was shown on August, 24th, during the one-day visit of the customer's director to Eindhoven. On 18th December, the final teleconference with discussion of the achieved results was held.

4.2. Money

The costs involved in the project include:

- TU/e budget for PDEng candidates.
- The project fee, paid by the customer to TU/e.
- The expected revenues (in long run) to the customer after selling the developed technology or patents, if such will be arranged.

TU/e has calculated the overall value of a 2-year PDEng Traineeship to be 250.000€ including tuition fees, trainings, salaries and office/equipment costs. The cost of the project for the principal is confidential and can not be mentioned in this report. However, it should be noted, that this amount is paid by the customer to TU/e for Maxim's work. Even rough estimation of possible revenues, brought by implementation of the proposed concepts and its introduction in the market of the marine propulsion systems, requires time consuming financial studies and calculation, which because of apparent

reasons can not be done in the framework of this project. However, to get insight into the possible benefits for the company, which is an owner of a unique technology, one may refer to the recently introduced Azipod (produced by ABB), the technology, which became a standard for modern cruise ships and brought to the company multi-million turnover.

4.3. Quality

The feasibility study should provide extensive and comprehensive data on the challenges of high-power high-speed permanent magnet motor design. To ensure the quality of the final report, four meetings with the industrial experts were held.

Phase	Activity to ensure quality	Responsible person
Initial	• Literature studies on the project topic.	Maxim
Definition	• Verification of the introduced design challenges by the experts in high-speed machines.	Maxim
Design	• Meeting with the head of CCM Dr. Frans Thoolen to discuss the maximal practical thickness of magnet enclosure for the rotor of high-speed motor. • Meeting with prof. van Terwisga to discuss new possible types of propulsors and its hydrodynamics efficiency. • Meeting with the industry expert at Advanced Electromagnetics (AE) to get a feedback on the concepts of new propulsors, presented in the final report.	Maxim and supervisors

Table A.2: List of activities performed to ensure quality in different phases.

4.4 Information

Phase	Document	Produced by	Recipient
Initial	Project assignment	Supervisors	Maxim
Definition	Project plan	Maxim and supervisors	Maxim and supervisors
Design	Preliminary report, presentations	Maxim	Supervisors
Realization	Final report, final presentation	Maxim	Supervisors, principal

Table A.3: Information exchange in different phases.

5. Organization

- Project owner.
- Contractor: head of the EPE group, prof. Dr. Elena Lomonova.
- Project leader: Dipl. Eng. Maxim Bogomolov.
- TU/e Supervisor: Dr. Johan Paulides, Dr. Aleksandar Borisavljevic.
- The working place of the author is located at EPE Group, TU/e.
- Meeting with representatives of the customer that took place in Netherlands, Eindhoven, TU/e.

6. Risk analysis

6.1 Risk list

Risk	Effect	Chance	Total	Selection
Delay in performing of all initial phase activities	1	2	2	
Slow progress because of the lack of knowledge in non-profile for EPE group subjects	2	2	4	X
Unavailability/unwillingness of industry experts in meetings	1	3	3	

Table A.4: List of risks.

6.2 Risk management

Due to the nature of the project, namely only the assessment of possible solutions for electrical propulsion, it is rather difficult to identify any possible risks which can

break planned sequence of project activities. In general, main risks are connected with the unexpected delay of performing all activities at the specific stage. As a result of such delays, it might be that not all of the required topics are covered by the final report. To manage these kind of risks, two extra margins are added in planning: before preliminary and final report. Due to the extra margins, the preliminary and final reports were delivered in time according to the initial schedule.

ID	Task Name	Start	Finish	Duration
1	Initial phase	2-4-2012	9-4-2012	6d
2	Compose technical proposal	2-4-2012	4-4-2012	3d
3	Define desired results and requirements	5-4-2012	9-4-2012	3d
4	Definition phase	9-4-2012	15-6-2012	50d
5	Define the requirements to the drive system	9-4-2012	20-4-2012	10d
6	Explore the benefits and drawbacks of electrical propulsion on ship	23-4-2012	25-5-2012	25d
7	Comparison of different types of electrical motors to be used for ship propulsion	28-5-2012	5-6-2012	7d
8	Make an overview of 20 MW high-speed motor design challenges	6-6-2012	15-6-2012	8d
9	Design phase	18-6-2012	24-8-2012	50d
10	Presentation for CCM	18-6-2012	25-6-2012	6d
11	Calculation of magnetic and electric loading	25-6-2012	6-7-2012	10d
12	Calculation of optimal magnet thickness	9-7-2012	17-7-2012	7d
13	Calculation of the gearbox dimensions	18-7-2012	3-8-2012	13d
14	Finalization of the preliminary report	3-8-2012	9-8-2012	5d
15	Presentation for the customer	13-8-2012	21-8-2012	7d
16	Margin	17-8-2012	24-8-2012	6d
17	Realization phase	27-8-2012	30-11-2012	70d
18	Presentation for MARIN	27-8-2012	17-9-2012	16d
19	Design of the machines with different power	18-9-2012	28-9-2012	9d
20	Determination of new conceptual propulsor's configuration	1-10-2012	19-10-2012	15d
21	Presentation for AE	22-10-2012	30-10-2012	7d
22	Finalization of the report	31-10-2012	28-11-2012	21d
23	Margin	27-11-2012	30-11-2012	4d
24	Improvement of the final report according to the remarks from the customer	3-12-2012	21-12-2012	15d

Figure A.1: Gannt chart.